The σ-hole interaction of 1,3-bis(2,6-diisopropylphenyl)imidazolidine [SiPr] with iodine-containing small molecules

By

Bradley H. C. Greene

A Thesis Submitted to

Saint Mary's University, Halifax, Nova Scotia

in Partial Fulfillment of the Requirements for

the Degree of Bachelor of Science

with Honours in Chemistry.

April 2016, Halifax, Nova Scotia

Approved: Dr. Jason Clyburne _____
Supervisor
Departments of Chemistry & Environmental Science

Approved: Dr. Robert Singer _____
Chairperson
Department of Chemistry

Date: April 1st, 2016

The σ-hole interaction of 1,3-bis(2,6-diisopropylphenyl)imidazolidine [SiPr] with iodine-containing small molecules

by Bradley H. C. Greene

Iodine-containing small molecules, such as R-CC-I and I-CC-I, can form halogen bonds, interactions that arise from the electrostatic forces between a halogen and Lewis base. This interaction arises from the presence of a σ-hole, an area of relatively positive electrostatic potential on the outer tip of the halogen. Halogens also have the ability to act as both halogen bond donors and acceptors in polyhalide environments. Our interest in N-heterocyclic carbene [NHC] chemistry led us to explore the reactivity of these strong C-centered bases with several iodine-containing small molecules, in particular, diiodoacetylene [ICCI] and 1- iodo-2-(trimethylsilyl)acetylene [ICC(TMS)]. We have systematically studied the reactions between the NHC, 1,3- Bis(2,6-diisopropylphenyl)imidazolidine [SiPr], and both the iodoalkynes and we have identified and characterized a variety of interesting products. For instance, we isolated SiPr•ICC(TMS) from the reaction with the TMS substituted acetylene. Perhaps the most interesting species were isolated from the interaction of SiPr and ICCI in the presence of excess iodide. [SiPr-I]I•ICCI•I[I-SiPr] and [SiPr-I]I•I_2CCI_2•I[I-SiPr] are unprecedented hybrid polyhalide species. Single crystal X-ray data have been collected for all of the products isolated. The structural geometries have been used to investigate the halogen bonding, and other intermolecular interactions, in these novel compounds.

April 1st, 2014

Acknowledgements

I would like to thank my honours supervisor, Dr. Jason Clyburne for all the opportunities he has given me during my time here at Saint Mary's. His passion and excitement for this discipline has enriched my time working for him. He has been inspiring. The guidance, understanding, and support he has provided has been endless and I am truly appreciative of it.

I would also like to thank Dr. Katherine Robertson. Her supervision and instruction while working in the Clyburne group has been invaluable. Her ability to handle an infinite amount of tasks at one time is unparalleled. This quality alone has shown me that even under the most stressful times things can be accomplished. I'd also like to thank her for her patience with me and willingness to help with anything I need, even if it is the furthest from her priorities.

I would like to thank members of the Clyburne group for their help and support throughout this research. Graeme Soper, Luke Murphy and Kirsten Doyle for their advice when I first began working here. I'd like congratulate fellow group members, Michael Land and Zoe Paula, on completing their honours and thank them for their support throughout this endeavour.

Thank you to the faculty and staff of the Saint Mary University Chemistry Department for the assistance in this research and other academic situations. Thank you to Elizabeth McLeod, Darlene Goucher, and Alyssa Doue for their resourcefulness. Special thanks to Dr. Jason Masuda for his expertise when I had problems with this research and Dr. John Young who was a supervisor on my first project and from whom I've learned so much.

Lastly, I would like to thank by family and friends for their unequivocal support and encouragement throughout this project and my time at Saint Mary's.

Table of Contents **Page**

List of Figures **Page**

List of Schemes **Page**

List of Tables **Page**

List of Symbols and Abbreviations

NHC	N-Heterocyclic carbene
ICCI	diiodoacetylene
ICC(TMS)	1-iodo-2-(trimethylsilyl)acetylene
HCC(TMS)	(trimethylsilyl)acetylene
SiPr	1,3-Bis(2,6-diisopropyl)imidazolidine
TMS	trimethylsilane
σ	sigma
XB	halogen bond
X	halogen
THF	tetrahydrofuran
HB	hydrogen bond
π	pi
HOMO	highest occupied molecular orbital
LUMO	lowest unoccupied molecular orbital
θ	theta
DCE	dichloroethane
DIPEA	diisopropylethylamine
hrs	hours
iPr	isopropyl
NMR	nuclear magnetic resonance
t-ButO$^-$	*tert*-butoxide ion
Ph_4B	tetraphenylborane
Å	angstrom
°	degrees
esd	estimated standard deviation
IR	infrared
K	Kelvin
iMes	1,3-bis(1,3,5-trimethylphenyl)imidazolidene
NIS	N-iodosuccinimide
DMF	dimethylformamide
α	alpha
β	beta
cm^{-1}	wavenumber
HPLC	high performance liquid chromatography
BHT	butylated hydroxytoluene
ACS	American Chemical Society
DCM	dichloromethane
d_n	deuterated
EA	elemental analysis
MP/mp	melting point
MHz	megahertz
g	gram

mmol	millimole
equiv.	equivalent
mL	milliliter
R.T.	room temperature
C	Celsius
mg	milligram
ppm	parts per million
δ	delta
d	doublet
s	singlet/strong
vs	very strong
m	multiplet/medium
Ar	aryl
w	weak
vw	very weak
Dec.	decomposition

1.0 Introduction

1.1 Halogen Bonding

The role of halogen atoms in chemistry is complex and extensive. Their typical chemical characteristics and reactivity are well-known. Maybe their most important characteristic is their one electron deficiency, which keeps them from having a complete octet of valance electrons. This results in their extreme reactivity, with an ability to form salts and also to form covalent bonds.[1] Their stability as ions also allows them to participate as Lewis bases in many reactions.[2] This is the typical view of the halogen atom, acting as a Lewis basic or nucleophilic compound, to form a covalent bond with a Lewis acid or an electrophile.

However, over the past 100 years, the interaction of halogens in donor-acceptor type situations has shown that their role can be quite versatile. Halogens have been proven to interact with nucleophilic species in numerous cases.[3,4,5] But why a typically electronegative, electron rich, Lewis basic species like a halogen, was susceptible to nucleophilic attack was still unclear.

Though such halogen interactions were first observed over a century ago, their true nature has only been discovered within the last 20 years.[5] It turns out that these interactions are very similar to hydrogen bonds, the most essential of the non-covalent bonds.[3] This similarity, along with even more useful characteristics, has resulted in a great deal of research interest, with emphasis on the general behaviour and the novel applications of these seemingly uncharacteristic interactions.[3]

1.1.1 History of Halogen Bonding

The first reported interaction of this type was found to occur between ammonia and iodine in 1914,[6] forming an iodoammonium complex which was isolated by Guthrie in 1983.[7] In 1911, Dehn reported that organic bases, such as trimethylamine, dipropylamine, and piperidine, formed complexes with carbon tetrabromide and diiodoacetylene (ICCI) in ether solutions.[8] He termed them “molecular aggregates” and claimed that their constant composition made them true molecular compounds. Benesi *et al.* (1948) noted interactions occurring between benzene derivatives and iodine, and used them as a potential explanation for changes in the absorption of iodine in solution.[9] The authors claimed that as the electron-donating ability of the substituents on the benzene ring increased, the interaction with iodine grew stronger.

During the 1950’s and 1960’s, Hassel *et al.* isolated and characterized numerous compounds of donor atoms, such as oxygen, with Br_2 (Figure 1).[10] According to Hassel *et al.*, the bromine atoms were acting as Lewis acids and accepting electron density from the oxygen donor atoms. They also noted that the O—Br—Br bond angles were very nearly linear in all cases. In 1968, Bent’s review on the nature of donor-acceptor interactions included a large number of compounds where halogen atoms acted as acceptor species.[11] Bent also suggested that these interactions were similar in strength to hydrogen bonds. Then, in 1983, the term “halogen bond” (XB) was first used to describe this type of interaction. Dumas *et al.* worked with compounds formed between carbon tetrahalides and Lewis basic compounds such as THF and pyridine.[12]

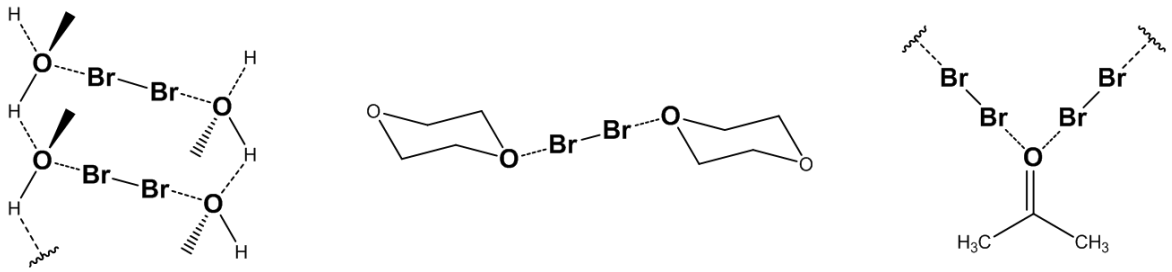

Figure 1: Methanol, 1,4-dioxane, and acetone complexes with Br_2 "molecular bridge" structures.[10]

. Investigation into the nature and application of the halogen interaction garnered a large amount of attention in the 1990's.[13] It was found that halogen bond donor ability followed the trend I > Br > Cl >> F, mirroring the halogen size and polarizability trends, while opposing that of electronegativity.[4, 14] It was also clear that, for the most part, XB donor ability was linked to the hybridization of the adjacent carbon atoms, and increased in the order $sp^1 > sp^2 > sp^3$.[14, 15, 24]

Finally, in early 1994 Politzer and Murray offered valuable insight into the theoretical understanding of the XB when they calculated the anisotropic distribution of electron density around covalently bonded halogen atoms.[16] They were the first to coin the term "σ-hole". In this model, electron density is drawn along the σ-C-X bond, resulting in an area of relatively positive electrostatic potential on the outer tip of the halogen atom. It is this area which is susceptible to attack by a Lewis base.

In 2001, Petrangelo and Resnati published a comprehensive summary of all the models, observations, and interactions reported to date.[5] This gave a unified model for the electrophilic behaviour of halogen atoms and as a result interest in the subject grew exponentially. Naturally, as interest has increased, studies into its potential applications

have increased as well (Figure 2). Today, reports of possible uses include self-assembly in crystal engineering.[17,18] incorporation into magnetic and conducting materials,[4] optical activity,[19] organocatalysis,[20] drug design and delivery,[21] biological recognition,[22] and liquid crystals.[23]

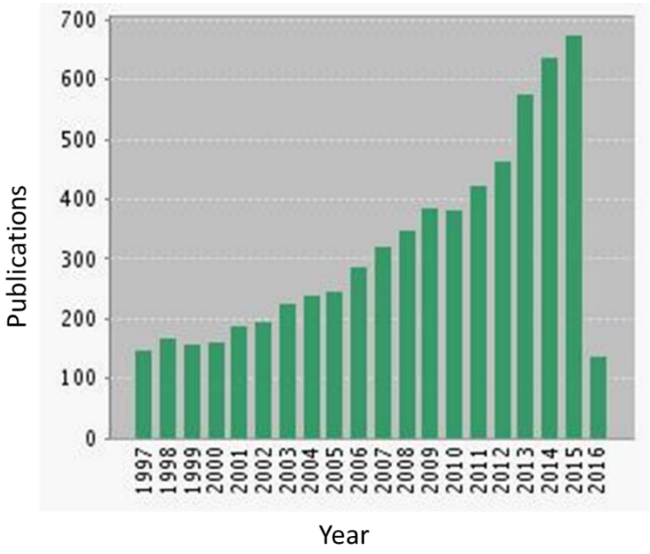

Figure 2: Publications per year containing the phrase “halogen bonding” (Source: Web Of Science: Accessed Apr 1 2016).

1.1.2 Nature of Halogen Bonding

Halogen bonding can be described as an attractive interaction between an electrophilic region on a halogen atom and a nucleophilic region of another atom. This type of interaction is quite different from the usual covalent bond in that involves the halogens.[1] In the XB interaction, the typically electron rich halogen atom is accepting electron density from a Lewis basic atom. It is, in fact, quite similar to another type of non-covalent bonding, hydrogen bonding (HB) (Figure 3).

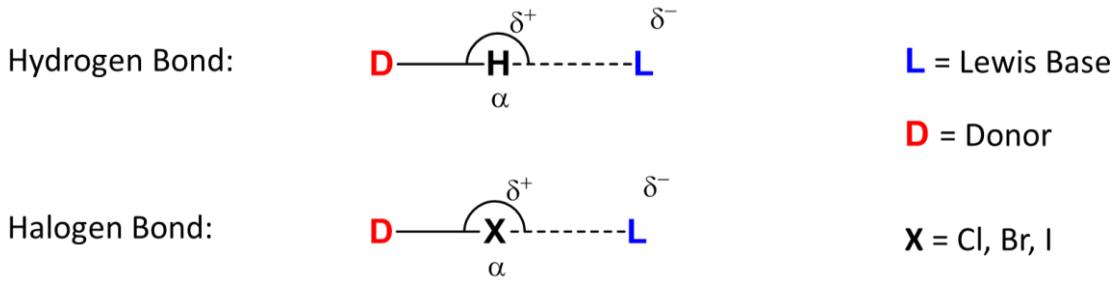

Figure 3: The similarity between halogen and hydrogen bonding.

As mentioned before, the strength of the bond is directly correlated to the size and polarizability of the halogen atom. The electrophilic region of the halogen atom is found to be on the outer tip of the atom, in line with the axis of the C-X bond. The remaining valence electrons lie in an outside (surrounding) ring, resulting in a large degree of directionality in the interaction.[14] Since the relatively positive electrostatic region lies on the tip, with the negative potential surrounding it, the strongest bonds are formed at angles near 180°.[3] This is observed in HB as well.[3]

The exact nature of the halogen bond is still open for some debate. However, the model proposed by Polizter in 1994 has undergone a fair amount of study and is the most widely accepted explanation for the interaction.[14,16] Typically, when a halogen forms a bond with another molecule, for example, carbon, it is done through a covalent bond, where electron density is shared through a σ-bond of overlapping orbitals on the halogen and carbon centres.[1] Now, in the case of a C-I bond, if another, more electronegative substituent is also bonded to the same carbon centre, electron density will be drawn away from the iodine atom through the σ-C-I bond.[3,4] This can be observed by viewing the electrostatic potential diagrams of CF_3X where X = F, Cl, Br or I (Figure 4).

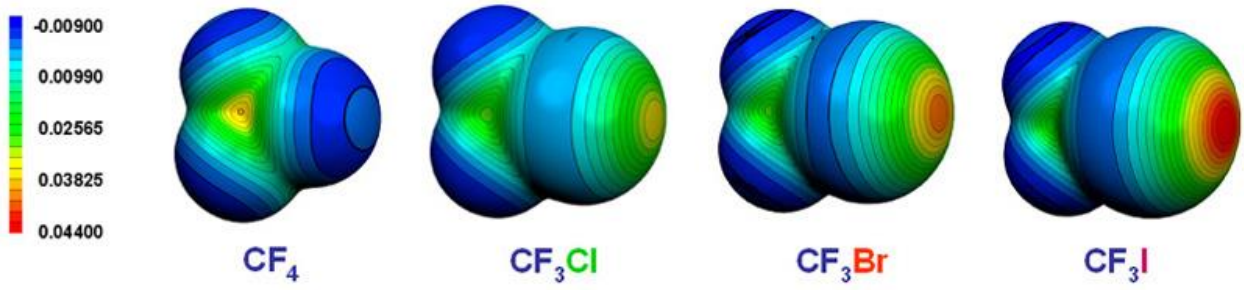

Figure 4: An electrostatic potential diagram of CF_3X, X = F, Cl, Br, I, showing the increasingly positive electron density on the tip of the halogen atom as the electronegativity of the unique halogen decreases.[3]

As the size and polarizability increases, and the electronegativity of the halogen atom decreases, the amount of electron density that can be drawn away increases.[25] Therefore, the size of the relatively positive region on the atom increases. It is this relatively positive region that is susceptible to nucleophilic attack and it is where the halogen bond interaction occurs.[3,16] It is also important to note that there is no "σ-hole" in CF_4, which strengthens this rationale.[4] The diagram also shows that there is a region of negative potential surrounding the relatively positive region. This is attributed to the remaining valence electrons in the π-orbitals of the halogen. This ring, or "equatorial belt", of negative potential creates directionality in the bond which has proven to be important in many applications.[3]

1.2 N-Heterocyclic Carbenes as Lewis Bases

Over the past few decades, carbenes have garnered a large amount of attention due to their applications in organometallic synthesis and catalysis.[26] The carbene can exist in two forms, the singlet and triplet states, with the former being more stable.[26,27] In the more stable singlet state, the carbene center bears a lone pair of electrons in a sp^2-

hybrized orbital while the *p*-orbital remains vacant. In the triplet state, two electrons of the same spin occupy different orbitals, either two *p*-orbitals or one *p*-orbital and one sp^2-hybridized orbital (Figure 5).

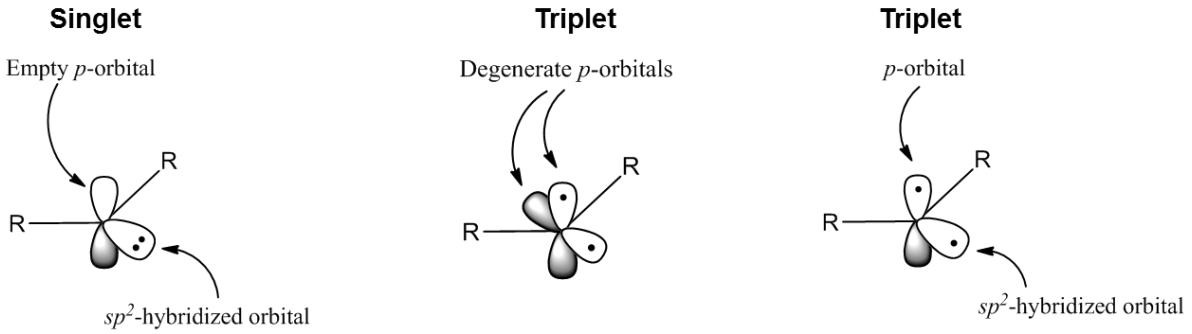

Figure 5: Orbital diagrams of singlet and triplet carbenes.

The N-heterocyclic carbenes have the carbenic carbon center positioned in an N-heterocyclic moiety.[28] These compounds have been known since the early 1960s, when Wanzlick investigated their reactivity through in situ studies.[29] However, it was not until 1991, that Arduengo first isolated a stable N-heterocyclic carbene.[30] Since then, research into their structures, properties and reactivity has significantly increased.[31]

The electronic nature of the NHC has garnered some debate.[28] At first, it was unclear as to whether or not electron density was being donated through π-orbitals from the lone pair of electrons in the nitrogen *p*-orbital to the empty *p*-orbital of the carbene center, forming an ylide type compound. Arduengo and Dixon initially determined, by mapping the electron distribution above the NHC plane and studying the length of the C-N bonds, that there was little contribution from the ylide form.[32,33] Later, however, Heinemann found that the stability indeed increased with delocalization of the π-electron

density between the nitrogen atoms and the carbene center. This stabilization is increased further when the backbone of the NHC is unsaturated.[34] When using a saturated NHC, electron density will be delocalized only through the carbenic center and the adjacent nitrogen atoms (Figure 6).

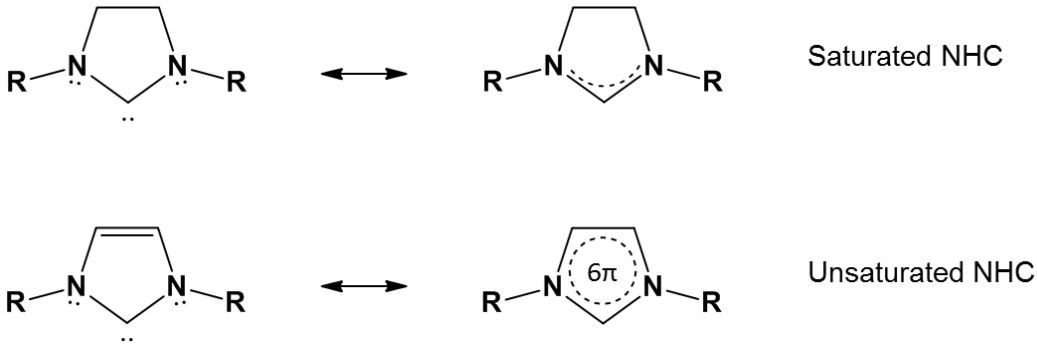

Figure 6: The difference in electron donation between π-orbitals in saturated and unsaturated NHC's.

In saturated NHCs, such as 1,3-bis(2,6-diisopropylphenyl)imidazolidine (SiPr), π-electron denisty is contained between the two nitrogen atoms and the carbenic carbon. Lone pair electrons in the *p*-orbital of the nitrogen atoms can be donated to the empty *p*-orbital of the carbon atom. This increases the HOMO-LUMO energy gap at the carbon atom and, hence, the triplet character of the carbene. This, in turn, decreases the stability of the carbene, which then increases its reactivity.

1.3 Iodoalkynes

The action of iodoalkynes with Lewis bases was first reported by Dehn, in 1911.[8] He studied their behaviour as Lewis acids when reacted with organic bases such as trimethylamine and dipropylamine. This reactivity was later studied further by Laurence *et al.* These authors used spectroscopic evidence to support the action of iodoalkynes as

Lewis acids. This was done using infrared spectroscopy and strongly suggested the formation of iodoalkyne-Lewis base complexes in solution.[35] In the 1960s, diiodoacetylene was also used to investigate the role of halogens in donor-acceptor interactions.[10,36,37]

Since that time, the role of iodoalkynes in halogen bonding has undergone a significant amount of scrutiny and these compounds have proven to be effective XB donors.[38,39,40] Typically, the strength of halogen bond donors are rationalized by having electron-withdrawing substiuents bonded to the same carbon atom as the halogen.[14] As the inductive electron-withdrawing ability of the group bonded to carbon increases, the ability of the halogen atom to participate in halogen bonding increases.[41] However, as mentioned before, it has also been reported that the ability of the XB donor changes as the hybridization of the adjacent carbon atom changes, in the order of $sp^1 > sp^2 > sp^3$.[8,14] This is important, as the iodoalkynes studied in this work offer no inductively coupled electron-withdrawing substituents. Hence, the presence of a σ-hole must be attributed to the hybridization of the carbon atom and also to the size and polarizabilty of the iodine atom.

The carbon-carbon triple bond of the acetylene functional group is comprised of a σ-bond and two π-bonds. Both carbon atoms form two sp^1-hybridized orbitals and contain two filled *p*-orbitals which are perpendicular to both the hybridized orbitals and each other. As the *s* character of the sp^1-hybridized orbitals increases, electrons tend to reside closer to the nucleus of the atom in question, due to the fact that the *s*-orbital is closer to the nucleus than the *p*-orbital.

A single iodine atom contains seven valence electrons, one shy of a full valence shell.[1] When hybridized, it forms four sp^3-orbitals, three of which each contain two electrons, while the fourth, the one potentially involved in bonding, contains one. The electons in these mainly *p*-character sp^3-orbitals are loosely held, contributing to their large degree of polarizability.

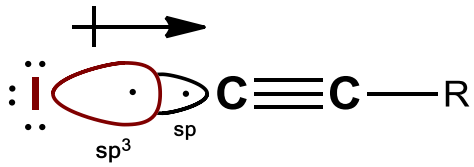

Figure 7: Polarization of the C-I σ-bond due to the size and shape of the *sp* and sp^3 orbitals involved in the bond forming orbital overlap.

When bond formation occurs between carbon and iodine, overlap of the carbon sp^1 orbital and the iodine sp^3 orbital ensues (Figure 7). Valence electrons on the iodine also reside in the much larger $5sp^3$-orbitals compared to the $2sp^1$-orbtials of carbon. Since the electron denisty is held close to the nucleus of the carbon atom, and the orbital of the iodine atom are so much larger, more electron denisty is donated from the polarizable $5sp^3$ orbital of the iodine atom in order to increase the strength of the bond. This creates a polar bond, and the polar bond is responsible for the σ-hole on the iodine.[40]

1.4 Iodine-Iodine Interactions

As is the case with XB, halogen-halogen interactions or bonding (C—X • X—C) can also be used as a design tool in supramolecular networks.[42] It was reported in 1963 that $C—X_1 • X_2—C$ contacts are found in two types of geometries.[43] Desiraju and Parthasarathy grouped the contacts with regards to the angles (θ) the interactions form,

with $\theta_1 = C_1—X_1 \bullet X_2$ and $\theta_2 = X_1 \bullet X_2—C_2$. They labelled them type I, where $\theta_1 = \theta_2$ and type II or bent, where $\theta_1 = 180°$ and $\theta_2 = 90°$ (Figure 8). Originally these types were more of a taxonomy, but a more recent publication by Desiraju studied the chemical basis behind the observed geometries. It was determined that there was a distinct difference in the geometries and chemical properties of compounds containing type I and type II interactions. Type I contacts arose from the close packing of molecules and occurred with all halogen atoms. It is not a halogen bond. Type II is a halogen bond, one that arises from an electrophilic-nucleophilic interaction. As the polarizability of the halogen increases, Cl < Br < I, the likelihood of a type II contact being formed increases as well.

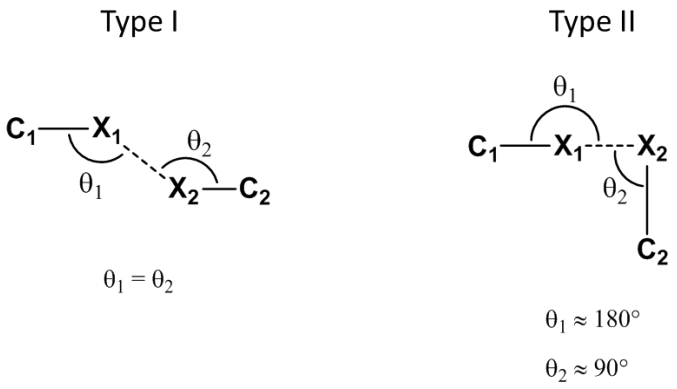

Figure 8: Type I and II X • X contacts

1.5 Objectives

In the 1990's, while Arduengo was completing the initial work on NHCs, he isolated several complexes formed between the NHCs and iodine containing compounds.[44,45] There have also been a few theoretical investigations into the action of NHC's in halogen bonding,[46] but very little experimental evidence has been provided. Figure 9 sums up most of what has been reported, experimentally, in the literature up to this point. The

characteristics NHCs possess, with regards to stability and reactivity, especially saturated NHCs, suggest that they could potentially play an important role as XB acceptors in many applications. Small iodine-containing molecules, and their interactions with a carbene, offer a favourable degree of simplicity that will allow a more fundamental investigation of the interaction, compared to more complex, organic systems.

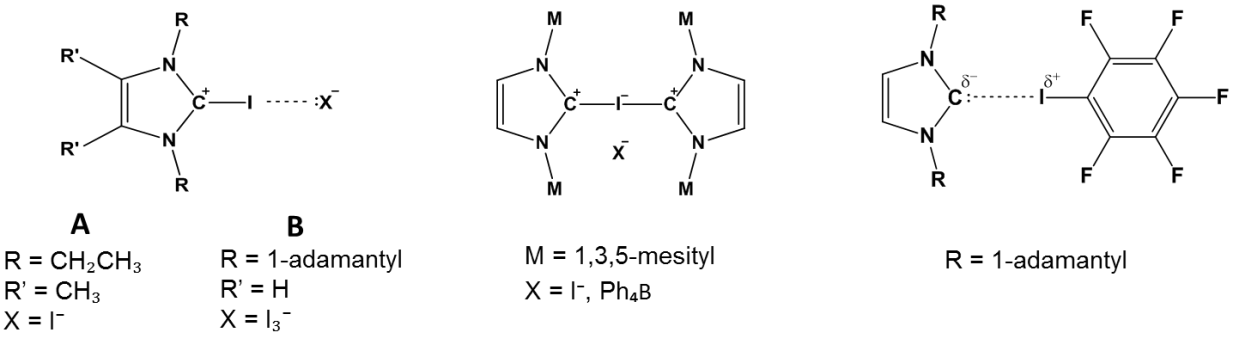

Figure 9: NHC • I(R) complexes isolated by Arduengo *et al*.[44,45]

It was decided to look at the role of the saturated NHC, SiPr, as a halogen bond acceptor in its interactions with both 1-iodo-2-(trimethylsilyl)acetylene and diiodoacetylene. There has been very little reported on the interaction of saturated NHCs with halogens in general. So, the interaction of SiPr with the above compounds in the presence of iodine will also be investigated.

2.0 Results and Discussion

The first goal of the project was to successfully synthesize a 1:1 adduct of SiPr and an iodoalkyne. Since members of the Clyburne group had previously worked with 1-iodo-2-(trimethylsilyl)acetylene (ICC(TMS)), this was chosen as the iodoalkyne to begin from. ICC(TMS) has only the alkyne substituent to act as an electron-withdrawing group. The lack of significant electron-withdrawing groups, such as fluorine, allows the nature of the σ-hole to be characterized based solely on the interaction between carbon and iodine. Since this compound is modest in cost and readily available, it was simply purchased from Sigma-Aldrich.

SiPr, however, is quite expensive to purchase and is only available in small quantities, so it was decided that it would be synthesized in house. This group has used a variety NHCs over the past few years. The total synthesis is a 3-step procedure, beginning with the synthesis of *N,N*-bis(2,6-diisopropylphenyl)formamidine. This procedure is outlined in Scheme 1.

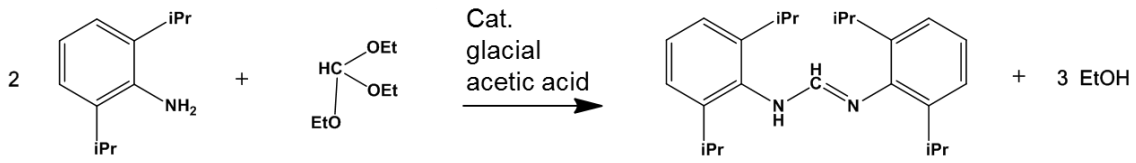

Scheme 1: Synthesis of *N,N*-bis(2,6-diisopropylphenyl)formamidine.[47]

Once the formamidine product has been isolated, step 2 in the SiPr synthesis is the preparation of *N,N*-bis(diisopropylphenyl)imidazolium chloride ([SiPr-H]Cl), through a ring-closing procedure using dichloroethane and diisopropylethylamine. This is outlined in Scheme 2. This reaction is run for 46 hours. One important step in this synthesis is the

separation of the desired product from the by-product, *N*,*N*-diisopropylethylamine. This is achieved with 3 x 100 mL triturations of the crude product with boiling toluene and significant stirring during the trituration. There is some loss of product but purification at this step is essential.

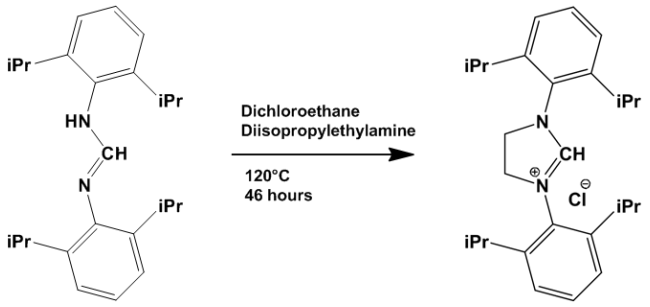

Scheme 2: Synthesis of [SiPr-H]Cl.[48]

The final step in the reaction sequence involves formation of the carbene. This is done via treatment of the chloride salt with sodium hydride and potassium *tert*-butoxide. Care must be taken when adding the sodium hydride as it is quite reactive. The reaction is done in THF and more THF, rather than less, should be used as the product is extracted into the THF solution. The product is also triturated with cold, dry hexanes to purify the final product. Formation and purification of the product should be confirmed by ^{1}H NMR analysis before proceeding further. The procedure is outlined in Scheme 3.

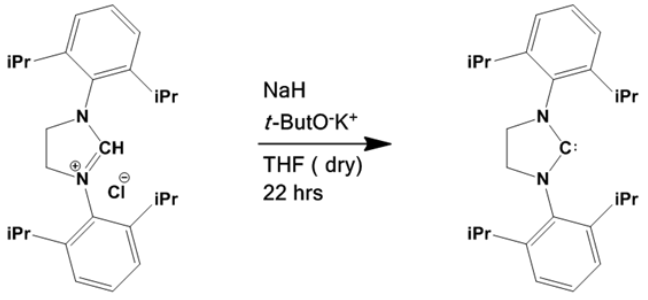

Scheme 3: Synthesis of SiPr.[49]

After successful synthesis of the carbene, preparation of the single adduct of SiPr onto the iodoalkyne was attempted. This was done on a micro-scale, due to the amount of time and effort needed to synthesize the starting materials. Equal molar equivalents of SiPr and ICCTMS were added to a small amount of benzene and allowed to react for 30 minutes. After the 30 minutes, the solvent was removed in vacuo and an off-white coloured powder was isolated. Infrared analysis showed that there had been a decrease in the frequency of the acetylene peak (Figure 10). This suggested that the desired product had been formed, as the interaction of iodine with SiPr should decrease the energy and frequency of the stretching peak and, hence, its wavenumber.

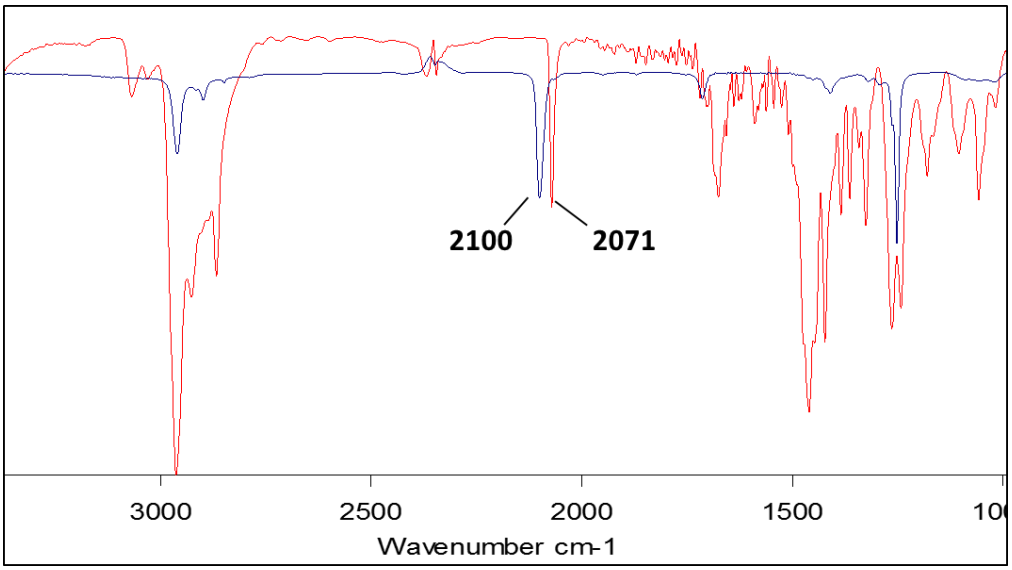

Figure 10: A comparison of the infrared spectra of SiPr•ICC(TMS), in red, and ICC(TMS), in blue, overlaid. Both were recorded as KBr pellets.

In a solution phase ^{13}C NMR spectrum, a peak at 225 ppm is observed and is assigned to the carbenic carbon. This peak is shifted from the reported peak of 244 ppm[59]. In a solid state ^{13}C NMR this carbenic carbon peak is not observed. We also observe a

slight shift in the I-C acetylene carbon peak from the reported value of 104 ppm[60] to our observed value at 98 ppm.

Obtaining crystals of the compound proved to be difficult. Originally attempts were made to crystallize the product via slow evaporation of the benzene solvent at room temperature. Through many attempts were made, no crystals were formed and it appeared that the compound was undergoing further reaction while still in solution. Though benzene contains no electron-withdrawing functional groups, its aromatic bond density is well-known to act as a nucleophile, especially with halogens.[9] This may offer some rationale for the further reaction of the SiPr•ICCTMS compound on standing in solution.

The halogen bond formed between the NHC carbenic carbon and the iodine, is expected to be a longer bond with less covalent character than a typical C-I σ-bond. It suggests that it is more of an interaction that occurs between the two reactants, rather than a bond-forming reaction. Mild conditions were chosen, including the use of a non-polar solvent, to deter any sort of solvent-reactant interaction, which could subsequently lead to further, unwanted reaction. Hexane was selected, and the reaction was carried out for only 30 minutes, with minimal stirring. The reaction flask was then immediately transferred to a freezer. After 2-3 hours, clear, colourless, rectangular, X-ray quality crystals formed in the flask containing the SiPr•ICC(TMS) product. Crystallographic data was collected for these crystals and the structure is shown in Figure 11.

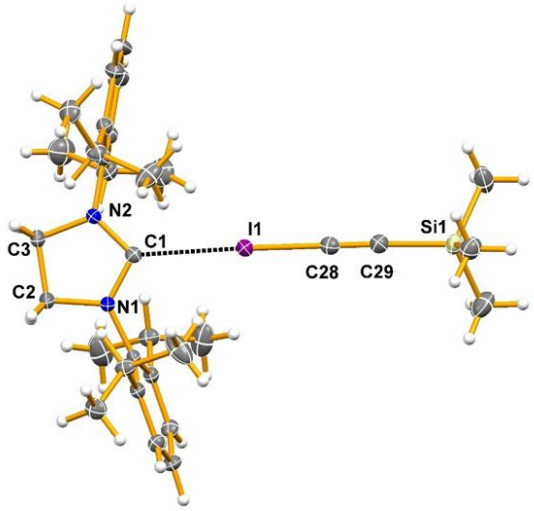

Figure 11: The crystal structure of SiPr•ICC(TMS). Thermal ellipsoids are drawn at the 50 % probability level. This, and all other, structural diagrams were prepared using the program Mercury as supplied by the Cambridge Crystallographic Data Centre.[50]

Table 1: Selected bond lengths and angles for SiPr•ICC(TMS).

Bond Length (Å)		**Bond Angle (°)**	
C1-I1	2.727(3)	C1-I1-C28	177.27(12)
I1-C28	2.083(4)	I1-C28-C29	178.2(3)
C28-C29	1.206(5)	N1-C1-N2	106.6(2)

Note: Atom numbering as depicted in Figure 11.

Selected bond lengths and angles for SiPr•ICC(TMS) are given in Table 1 above. The bond lengths for C1-I1, I1-C28, and C28-C29 suggest that a halogen bond has been formed between the Lewis basic carbenic carbon atom with the σ-hole on the iodine atom. The longer length of the C1-I1 bond compared to that of I1-C28, suggests that the latter is stronger, with more covalent character. The former seems to be more characteristic of a weaker electronic interaction, with electron density being donated from the carbene to

the sigma-hole of iodine. The bond angles are also supportive of a sigma-hole type interaction being present in the structure. Ideally, as is the case in hydrogen bonding,[14] angles of or near 180° offer the strongest interactions.[14]

Weak hydrogen bonding contacts (C-H…I) in the same compound also offer support as to the existence of a σ-hole. As mentioned in the introduction, the sigma-hole is produced from electron density being drawn through the σ-bond axis towards the carbon atom. This still leaves valance electrons in the remaining sp^3-hybridized orbitals, which form an equatorial belt of negative electrostatic potential around the iodine atom. Therefore, it makes sense that this belt of negative potential could act as an acceptor for hydrogen bonds, and this is what is observed (Figure 12).

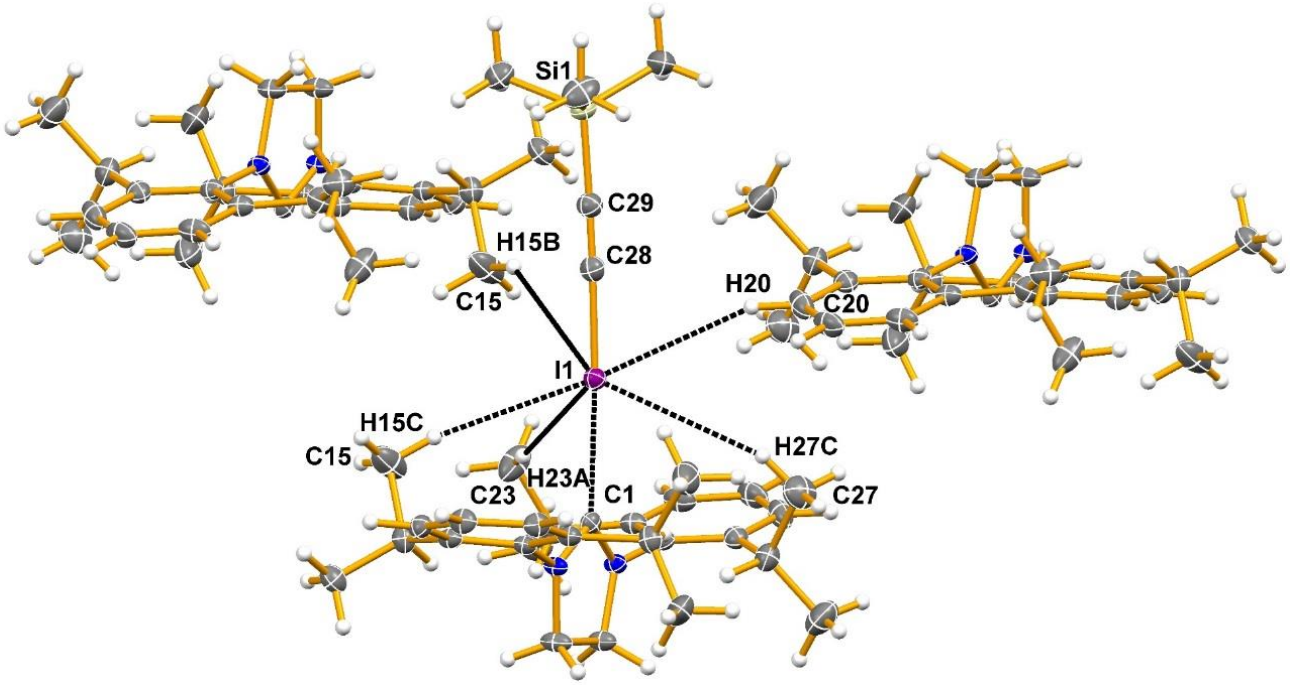

Figure 12: Weak C-H…I type contacts to iodine in the SiPr•ICC(TMS) crystal structure.

Table 2: C-H…I contacts in SiPr•ICC(TMS), with I1 acting as the acceptor in every case.

H…I Distance (Å)		**C-H…I Angle (°)**	
C15 - H15B	3.46	C15-H15B…I1	142.1
C15 - H15C	3.21	C15-H15…I1	167.2
C23 - H23A	3.20	C23-H23A…I1	153.8
C27 - H27C	3.46	C27-H27C…I1	159.1
C20 - H20	3.24	C20-H20…I1	157.9

Note: Atom numbering as depicted in Figure 12. Esds are not reported as the hydrogen atoms were placed in geometric positions and not refined.

Since we could now successfully synthesize SiPr•ICC(TMS), an attempt was made to prepare the bis-adduct of SiPr to diiodoacetylene (ICCI). A means other than the reaction of two equivalents of SiPr with one equivalent of ICCI was chosen. It was hoped that the reaction of SiPr•ICC(TMS) with [SiPr-I]I might displace (TMS)I leaving the bis-adduct. NHC • I_2 type interactions have been documented previously.[45] In our reaction, SiPr was first stirred with iodine for 10 mins in benzene. In a second flask, SiPr was stirred with ICC(TMS) for 10 minutes in benzene. Subsequently, the two solutions were combined and left to react for 30 minutes.

The bis-adduct was not formed. However, the [SiPr-I]I product was isolated and successfully characterized using IR, NMR and crystallographic analysis (Figure 13). [SiPr-I]I was compared to the other NHC • I_2 compounds that had been reported and the bond lengths and angles, IR, and NMR data are in good agreement.[45] It is interesting to note the differences in the C1-I1 and I1-I2 bond lengths (Table 3). The C1-I1 bond length

is much shorter than that of I1-I2, suggesting the former is more of a covalent bond while the latter is a donor-acceptor interaction. This is contrary to the results reported in Bent's review of donor-acceptor interactions. In this, he reports that complexes are formed in which the I—I bond is more covalent while the Lewis base-I bond is more of a donor-acceptor interaction. Therefore, it is likely that saturated NHC's differ in their roles as halogen bond acceptors. It appears that the NHC forms a stronger, more covalent bond with I1, creating a sigma-hole. Then you have I2 behaving as the halogen bond acceptor instead of the NHC.

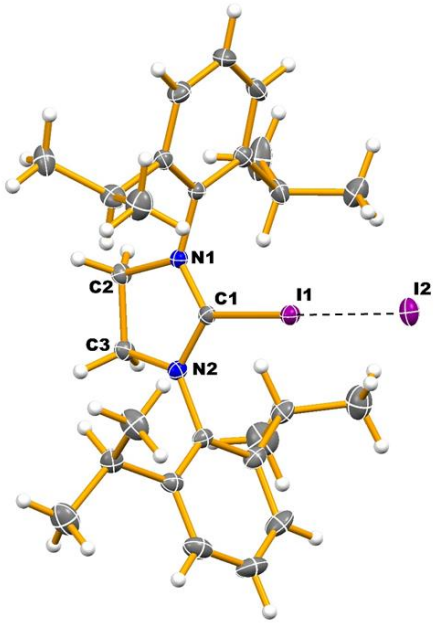

Figure 13: The crystal structure of [SiPr-I]I at 125 K.

Also note that the bond angle C1-I1-I2 is very nearly linear. This, along with the bond lengths, supports the claim of a halogen interaction occurring between the NHC-I XB donor and the iodide ion XB acceptor.

Table 3: Selected bond lengths and angles of [SiPr-I]I.

Bond Length (Å)		**Bond Angle (°)**	
C1-I1	2.124(4)	C1-I1-I2	175.85(10)
I1-I2	3.2438(9)	N1-C1-N2	112.5(3)

Note: Atom numbering as depicted in Figure 13.

As mentioned earlier, the XB shows many similarities to the HB. Therefore, the crystal structures of [SiPr-I]I and [SiPr-H]I (Figure 14) were compared. As you can see from Table 4, the H1-I1 bond length is shorter than that of the I1-I2 bond length, which is expected. However, both compounds appear to interact in the same fashion. With SiPr forming a covalent bond with either I or H and then behaving as either a hydrogen or halogen bond donor.

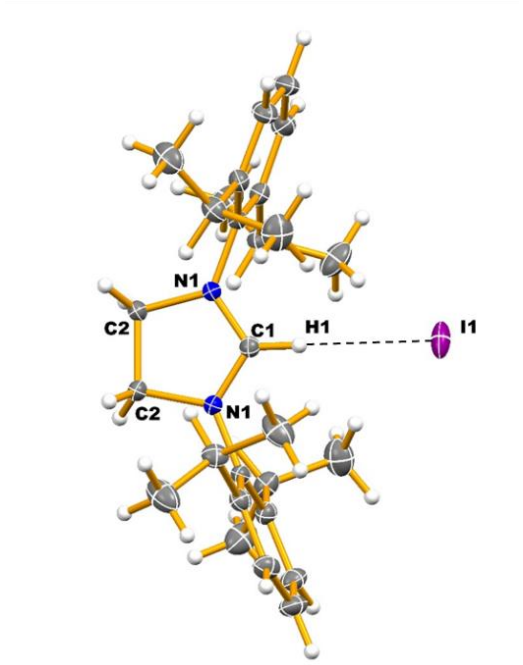

Figure 14: The crystal structure of [SiPr-H]I at 125K.

Table 4: Selected bond lengths and angles of [SiPr-H]I.

Bond Length (Å)		**Bond Angle (°)**	
C1-H1	0.96(3)	C1-H1-I1	180.000(1)
H1-I1	2.75(3)	N1-C1-N2	113.3(2)

Note: Atom numbering as depicted in Figure 14.

As mentioned earlier, obtaining crystals of SiPr•ICC(TMS) took some time and proved to be quite problematic. It was found that if the solvent was removed in vacuo, the solid product immediately decomposed. It was also determined that if left in solution for slow evaporation at room temperature, the complex would undergo further reaction to produce a variety of new products. Some of these products could be isolated and were characterized using X-ray crystallography and, when possible, NMR analysis.

One complex was isolated which contained a SiPr—I—SiPr cation along with 2 ICCI molecules, an iodide ion and a benzene solvent molecule (Figure 15). This complex was formed when a 1:1 ratio of SiPr was added to ICC(TMS). The reaction was carried out at room temperature for 30 minutes in either benzene or THF. The solutions were then left to evaporate and crystals were collected. From both reactions, crystals with similar structures were isolated, differing only in the solvent incorporated into the crystal. A bis-adduct of 1,3-bis(1,3,5-trimethylphenyl)imidazolidene (iMes) to a single iodide atom was reported by Arduengo *et al.* in the early 1990's. The two C-I bond lengths in the compound he reported were 2.286(4)Å and 2.363(4)Å, while the C-I-C bond angle was 177.5(2)°.[45] The C1-I1 bond length and the C1-I1-C2 bond angle in our structure are almost in exact agreement with those reported by Arduengo (Table 5). There was a difference, however, in the N-C-N bond angles. Those reported in Arduengo's compound

were 105.3(4)° and 106.2(4)°, while the N-C-N angle for both carbene units in our structure was 108.7(5)°. This is expected as Arduengo used an unsaturated carbene, resulting in more electron density being contained within the ring and tightening that bond. The complex that is formed between the two ICCI molecules and the iodide has also been reported with a tetraphenylphosphium cation instead of the SiPr-I-SiPr cation.[51] This complex has also been isolated and it was found that the anionic moiety is quite similar in both of our compounds.

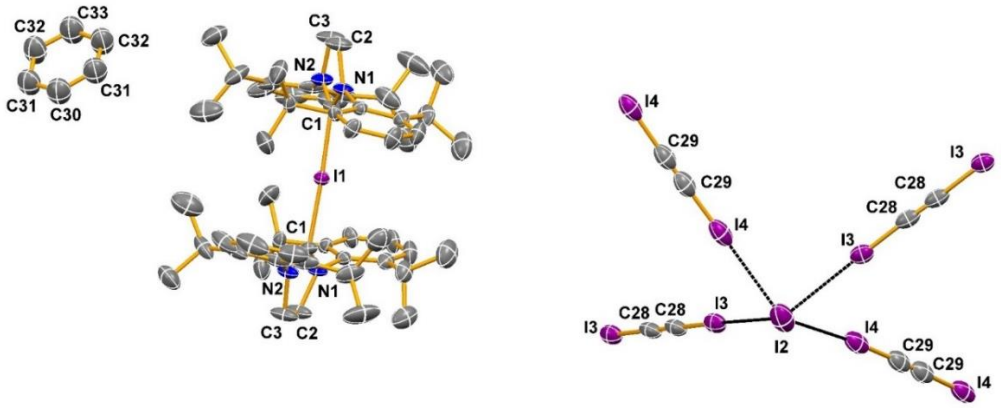

Figure 15: The crystal structure of [SiPr-I-SiPr]I•[ICCl]$_2$•C_6H_6 at 125 K.

Table 5: Selected bond lengths and angles of [SiPr-I-SiPr]I•[ICCl]$_2$•C_6H_6.

Bond Length (Å)		**Bond Angles (°)**	
I1-C1	2.337(6)	C1-I1-C1	177.5(3)
I2-13	3.4865(9)	C28-I3-I2	175.9(3)
I2-I4	3.4900(11)	C29-I4-I2	178.2(3)
C28-I3	1.966	I3-I2-I3'[a]	136.6[c]
C29-I4	2.048	I4-I2-I4'[b]	135.2[c]
--	--	N1-C1-N2	108.7(5)

Note: Atom numbering as depicted in Figure 15. (a) I3 and I3’ are symmetry equivalent atoms. (b) I4 and I4’ are symmetry equivalent atoms. (c) Esds are missing because the refinement has not been finalized.

The bond lengths shown are almost an exact match to those found in the related tetraphenylphosphonium salt.[51] In this structure, it is important to note the bond angles between I2, I3, and I4 and the roles of those atoms as halogen bond donors and/or acceptors. The I3-I2-I3’ and I4-I2-I4’ angles, at 136.6° and 135.2°, respectively, are quite small for σ-hole type interactions. In contrast, the bond angles C28-I3-I2 and C29-I4-I2 are nearly linear and much more characteristic of a halogen bond interaction. This suggests that electron density from the lone pair of electrons in the sp^3-hybridized orbitals of the iodide anion is being donated to the neighbouring σ-hole of the iodine in the ICCI molecules. I2 acts as a XB acceptor, while I3 and I4 act as XB donors.

SiPr and ICC(TMS) were also reacted under somewhat different conditions by a previous member of the Clyburne group. In one case, the reactants were added to toluene and refluxed for 1 hour. The resulting dark black slurry was washed with pentane and filtered through alumina. The solution was left to evaporate at room temperature and crystals formed. A SiPr•ICCI•SiPr complex was isolated and characterized by X-ray diffraction and NMR (Figure 16). This procedure was repeated numerous times to try and recover the bis-adduct but to no avail. It was decided that it might be better to isolate the same product from the reaction between two equivalents of SiPr and 1 equivalent of ICCI.

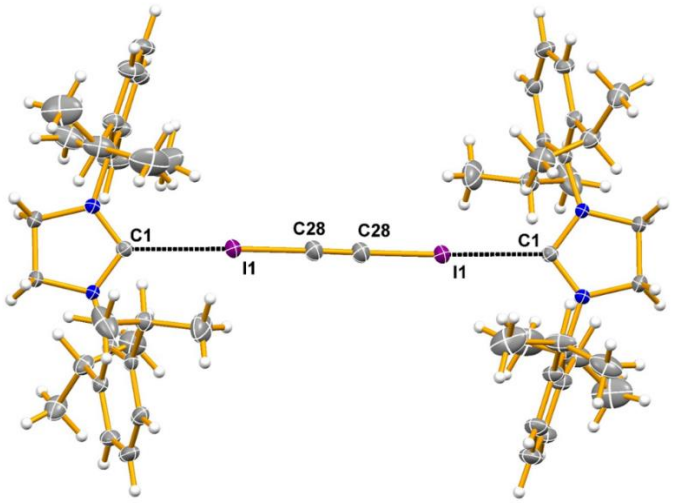

Figure 16: The crystal structure of SiPr•ICCI•SiPr at 125 K.

ICCI had to be synthesized as it was not available commercially. A previously reported synthesis of this compound involves the use of acetylene gas, which has numerous safety concerns.[52] Conveniently, another synthesis had been reported by Perkins *et al.* (Scheme 3)[53]. This one involved the use of *N*-iodosuccinimide (NIS) and trimethylsilylacetylene (HCC(TMS)). This was the procedure followed. NIS, HCC(TMS) and silver nitrate were added to dimethylformamide (DMF) and reacted at room temperature for one hour. The resulting solution was then treated with deionized water and washed with diethyl ether. The diethyl ether layer was separated and dried with magnesium sulfate. ICCI emits a very strong odor and all work must be done in a fume hood once it has been removed from the glovebox. Since ICCI has been reported to decompose violently at temperatures between 80-130°C or due to shock, it was kept in solution and only handled as a solid with great care. Due to its reactivity in the solid state, an exact concentration was never obtained. An approximate concentration was calculated, assuming that 90% conversion had occurred. There also appeared to be an

issue in this synthesis with the presence of excess iodine or iodide. This problem became apparent when SiPr was reacted with the ICCI solution.

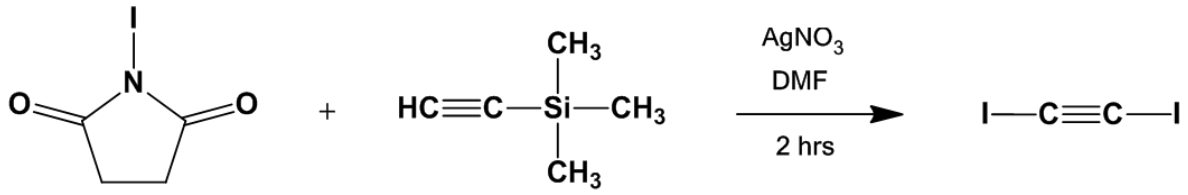

Scheme 3: The synthesis of ICCI.[53]

The reaction to produce the bis adduct of SiPr with ICCI was carried out in a number of different solvents. Originally the reaction was completed in diethyl ether, simply because the ICCI was stored in that solvent. SiPr was added to the ether and stirred, then the ICCI solution was added dropwise. A precipitate formed immediately upon the addition of the ICCI solution. The reaction was left to proceed for 30 minutes, at which time the precipitate was filtered off using gravity filtration. The precipitate was then treated with acetonitrile, which dissolved the majority of the solid. The undissolved solid was removed using gravity filtration and dissolved in dichloromethane. The three solutions were left to slowly evaporate.

Clear, rectangular, X-ray quality crystals were obtained from the acetonitrile solution. X-ray data was collected and a [SiPr-I]I•ICCI•I[I-SiPr] complex was characterized (Figure 17).

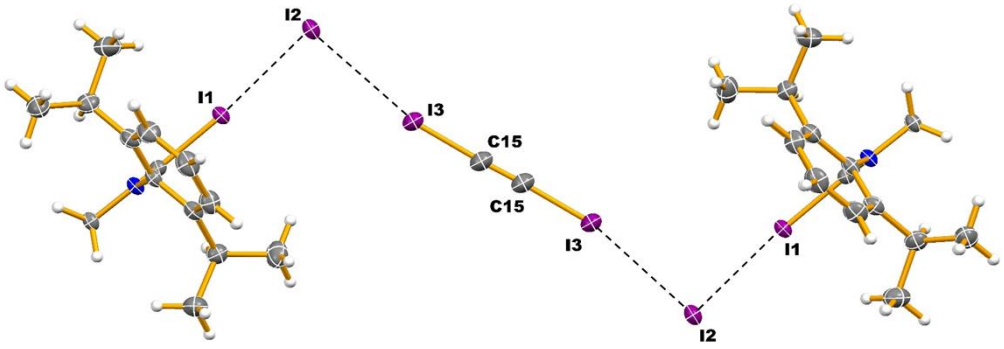

Figure 17: The crystal structure of [SiPr-I]I•ICCI•I[I-SiPr] at 125K.

Table 6: Selected bond lengths and angles in [SiPr-I]I•ICCI•I[I-SiPr]

Bond Length (Å)		**Bond Angle (°)**	
C1-I1	2.110(4)	C1-I1-I2	176.16(10)
I1-I2	3.193(1)	I1-I2-I3	94.07(2)
I2-I3	3.520(1)	I2-I3-C15	168.02(14)
I3-C15	2.023(5)	I3-C15-C15	177.6(6)
C15-C15	1.202(9)	N1-C1-N2	112.7(5)

Note: Atom numbering as depicted in Figure 17.

The complex consists of two [SiPr-I]I components, coordinating to a single ICCI molecule. When comparing the structure of the [SiPr-I]I portion of this compound with that of the solo [SiPr-I]I compound there are some notable differences. The C1-I1 bonds in both are similar at 2.110(4) Å and 2.124(4) Å, respectively. However, the I1-I2 bonds are quite different. For the complex mentioned above, this bond is 0.47 Å longer than the same bond in the solo compound, suggesting that I1 is, again, acting as a XB donor. The change in length of I1-I2 bond from the [SiPr-I]I compound can be rationalized by inferring

that there is also electron donation by I2 into the sigma-hole of I3, which decreases the strength of the I1-I2 bond and, therefore, increases its length. The I2-I3 contact is longer than all of the other bonds in the complex. However, it is comparable in length to the I…I interaction in the previously discussed compound. This supports the idea that this is a form of halogen bonding, with I3 acting as the XB donor. The bond angles of both C1-I1-12 and I2-I3-C15 are nearly linear, which helps support the previous claim.

Comparison of the infrared spectra of [SiPr-I]I•ICCI•I[I-SiPr] and [SiPr-I]I also offers support as to the existence of the bis-adduct to ICCI (Figure 18). The presence of a peak at 671 cm^{-1} is indicative of a terminal ≡C-I stretch in the former. This peak is not observed in the spectrum of [SiPr-I]I; this is further evidence supporting the formation of the bis adduct.

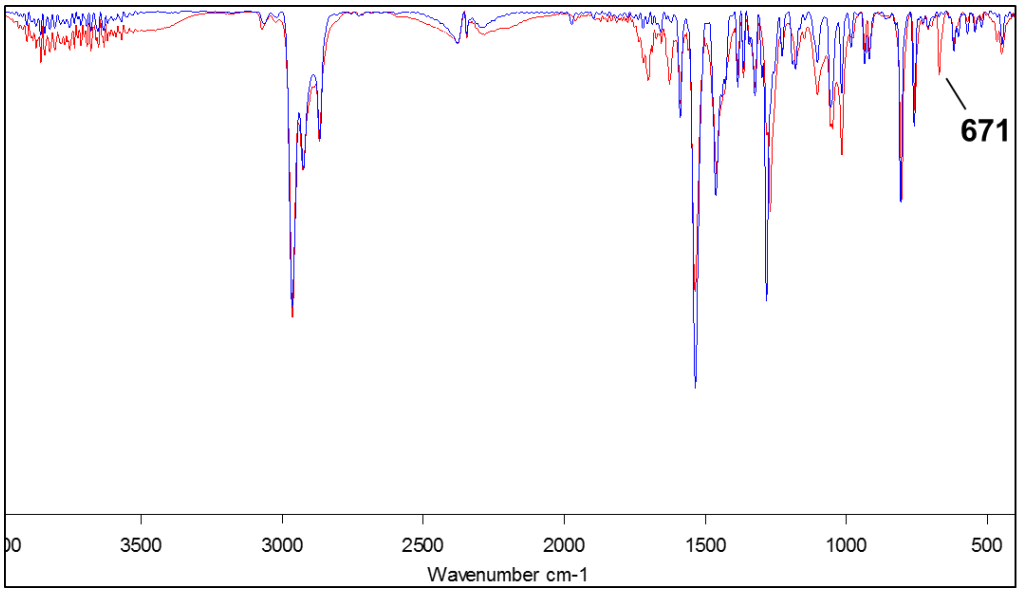

Figure 18: Infrared spectra of [SiPr-I]I, in blue, and [SiPr-I]I•ICCI•I[I-SiPr], in red, overlaid. Spectra were recorded as KBr pellets.

This molecule also offers the possibility of some interesting applications. Since the complex SiPr•ICCI•SiPr (Figure 16) was isolated previously by another member of the

Clyburne group, we know for certain that it exists. Therefore, there is potential for the [SiPr-I]I•ICCI•I[I-SiPr] compound to act as a oxidizing agent through the loss of iodine.

The above compound was isolated quite regularly from the reaction of SiPr with the ICCI solution. It is possible that there was an excess of iodide in the solution. This iodide would quickly react with SiPr forming the [SiPr-I]I salt, which could then coordinate to the ICCI forming the bis-adduct. Thus, a sequence of small additions of SiPr was made to the ICCI solution in an attempt to quench the excess iodide. It was assumed that the [SiPr-I]I•ICCI•I[I-SiPr] compound would form, and precipitate out of solution upon formation. The remaining solution would be decanted off and again reacted with more SiPr. This step would be repeated until nothing precipitated upon the addition. The resulting solution would be left to crystallize, with the hope that the SiPr•ICCI•SiPr compound would be formed. The solid that did precipitate out was dissolved in acetonitrile and allowed to crystallize through slow evaporation. X-ray quality crystals were obtained and an unexpected compound was isolated (Figure 19).

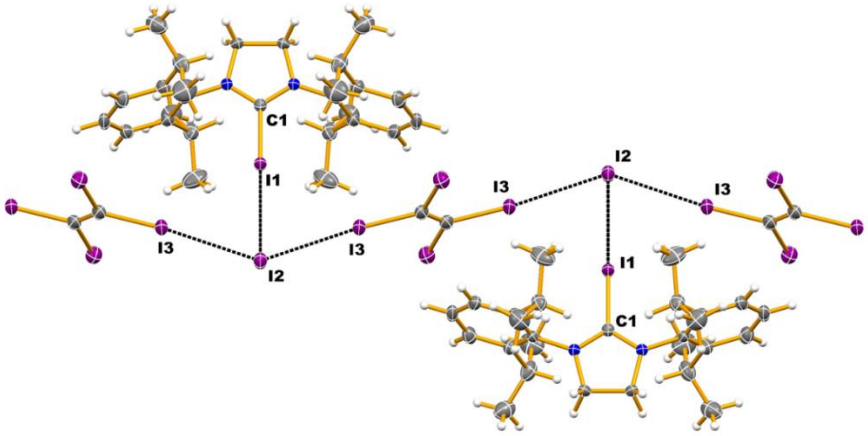

Figure 19: The crystal structure of [SiPr-I]I•I_2CCI_2•I[SiPr-I] at 125K highlighting the iodine-iodine interactions.

Table 7: Selected bond lengths and angles of [SiPr-I]I•I_2CCI_2•I[SiPr-I]

Bond Length (Å)		**Bond Angle (°)**	
C1-I1	2.094(5)	C1-I1-I2	178.98(13)
I1-I2	3.3960(5)	I1-I2-I3	72.52(1)
I2-I3	3.4146(3)	I2-I3-C15	175.23(11)
I3-C15	2.109(4)	I3-C15-C15	123.8(4)
I4-C15	2.106(4)	I4-C15-C15	122.6(4)
C15-C15	1.327(8)	N1-C1-N2	113.0(4)

Note: Atom numbering as depicted in Figure 19.

Similar to the [SiPr-I]I•ICCI•I[I-SiPr] compound, it appears that I2 is again acting as a XB acceptor from both I1 and I3. The I1-I2 and I2-I3 bond lengths are significantly longer than those of C1-I1 and I3-C15, suggesting the latter are bonds of more covalent character, while the former interactions are electrostatic in nature. The bond angles are also supportive of the idea that a XB has been formed between I1-I2 and I2-I3, with both C1-I1-I2 and I2-I3-C15 being near linearity. The I1-I2-I3 bond angle is also in agreement with what has previously been explained about type II halogen-halogen contacts. I4 in this compound is also involved in a π-type interaction with the electron density in one of the phenyl rings on the carbene compound (Figure 20). It is likely that this interaction strengthens [SiPr-I]I•I_2CCI_2•I[SiPr-I] in the solid state, since the XB between I2 and I3 is weaker than that of [SiPr-I]I•ICCI•I[I-SiPr].

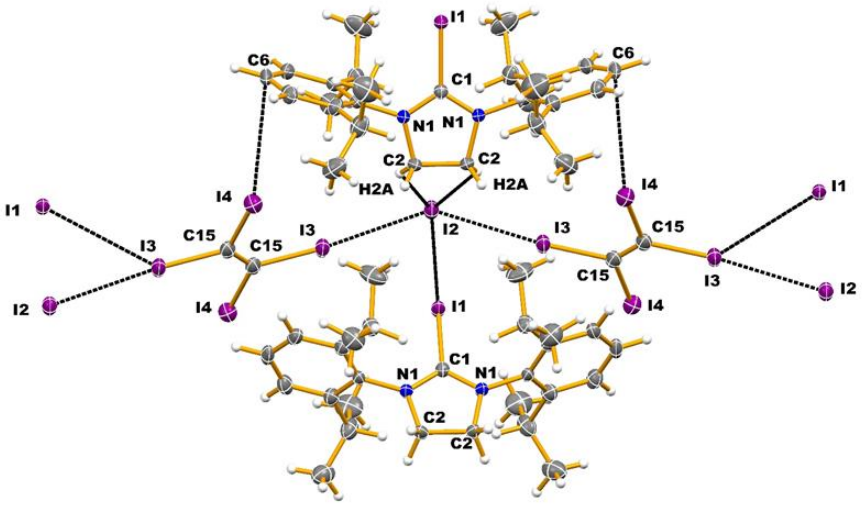

Figure 20: The crystal structure of [SiPr-I]I•I_2CCI_2•I[SiPr-I] at 125K showing selected intermolecular contacts.

Interesting results arise when we compare the common bonds and angles in this compound to both [SiPr-I]I•ICCl•I[I-SiPr] and [SiPr-I]I (Table 8). (For this comparison [SiPr-I]I•I_2CCI_2•I[SiPr-I], [SiPr-I]I•ICCl•I[I-SiPr], and [SiPr-I]I have been denoted by **1**, **2**, and **3**, respectively. The C1-I1 bond lengths increase in the order of **1** < **2** < **3** and the distances decrease in the same order for the I1-I3 bonds. The I2-I3 bond length, which does not apply to **3**, is shorter in **1** than in **2**. The exact reason for these observations has not yet been fully determined but a rationale will be offered. I3 in **1** is covalently linked to C15 by overlap of the iodine sp^3-orbital and the carbon sp^2-orbital. Since the hybrid orbital on this carbon has more *p*-character than C15 in **2**, less electron donation from I3 is needed to form the bond. This results in a smaller σ-hole on I3 in **1**. It would seem that this would result in a longer I2-I3 bond for **1** than **2** since the σ-hole is smaller in **1**. However, we see a shorter I2-I3 bond length in **1** than **2**. A reasonable basis to explain the trend is the "trans-effect" proposed by Knop *et al*[58] which describes a connection

between adjacent bond lengths of atoms of the same element. In **1** the I3-C15 is longer than the I3-C15 in **2**. Then you have a shorter bond for I2-I3 in **1** than **2**. Then you have a longer bond for I1-I2 in **1** than **2** and, finally, a shorter C1-I1 bond length in **1** than **2**. The fact that I2 in **1** forms contacts with three iodine atoms while I2 in **2** only forms two contacts, may also play a role. The I1-I2 bond in **3** falls in the middle of **1** and **2**, so a rationale involving the influence of the sigma hole on I1 does not make sense. The influence of the size of the σ-hole could still have some role in the observed trend, however, more investigation is needed. One observation that does support the change in the σ-hole from **1**, which would be smaller, and **2**, is the angle of the I2-I3-C15 bond. Since the σ-hole on I3 in **1** is smaller than that on **2**, the bond angle needs to be more linear in **1**. In **2** the σ-hole on I3 is larger, therefore the I2-I3-C15 bond angle can vary from linearity and still form the XB bond and this what is observed. The decrease in the I1-I2-I3 angle from **2** to **1** is possibly due to electronic effects on the adjacent iodine, I4, in **1**, which is not present in **2**.

Table 8: Comparison of selected bond lengths and angles of [SiPr-I]I•I_2CCI_2•I[SiPr-I] (**1**), [SiPr-I]I•ICCI•I[I-SiPr] (**2**), and [SiPr-I]I (**3**).

Bond Length (Å)				**Bond Angle (°)**			
	1	**2**	**3**		**1**	**2**	**3**
C1-I1	2.094(5)	2.110(4)	2.124(4)	C1-I1-I2	178.98(13)	176.16(10)	175.85(10)
I1-I2	3.3960(5)	3.193(1)	3.2438(9)	I1-I2-I3	72.52(1)	94.07(2)	--
I2-I3	3.4146(3)	3.520(1)	--	I2-I3-C15	175.23(11)	168.02(14)	--
I3-C15	2.109(4)	2.023(5)	--	I3-C15-C15	123.8(4)	177.6(6)	--
C15-C15	1.327(8)	1.202(9)	--	N1-C1-N2	113.0(4)	112.7(5)	112.5(3)

Note: Atom numbering for **1**, **2**, and **3** are as depicted in Figures 19, 17, and 13, respectively.

Lastly, little was found in the literature on the interactions of saturated NHCs and iodine. Preparation of such a polyiodide complex could provide valuable information on the behaviour of polyhalides and their potential applications. Therefore, attempts were made to prepare a polyiodide/SiPr complex and these were somewhat successful. A $[SiPr]_2 \bullet [I]_{16}$ complex was isolated and found to contain I^-, I_2, and I_3^- moieties using X-ray crystallography (Figure 21).

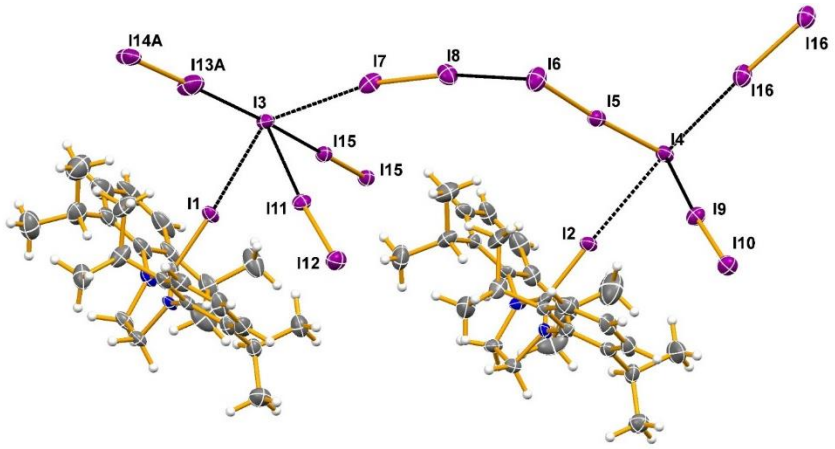

Figure 21: The crystal structure of the SiPr polyiodide complex at 125K.

Again, as can be seen from the contacts shown in the diagram, iodine exhibits the ability to act as both a halogen bond donor and acceptor. The SiPr-I cation acts as a halogen bond donor, which is the case in other of the compounds discussed above. It appears that the negatively charged iodine species act as the halogen bond acceptors. Iodine acts as a halogen bond donor, which is in agreement with work published by Hassel and Bent.[10, 11]

There is a common trend observed in the behaviour of the carbenic N1-C1-N2 bond angle (Table 9). Interpretation of this trend could offer valuable insight into the nature of the halogen bond formed between an NHC and iodine. Bond angles for this particular

segment of the carbene increase in the order SiPr•ICC(TMS) < [SiPr-I-SiPr]I • $[ICCl]_2$ < [SiPr-I]I ≈ [SiPr-I]I•ICCl•I[I-SiPr] ≈ [SiPr-I]I•I_2CCI_2•I[SiPr-I] < $[SiPr\text{-}I]_2[I]_{16}$. This can be rationalized by looking at the electronic environment of the central carbon atom. In the compounds with the largest bond angles, a [SiPr-I] cation is formed with a shorter C-I bond length. This suggests that a covalent bond is formed, with the carbon centre bonding to the iodine through an sp^2-hydridized orbital (Figure 22). In the SiPr-I-SiPr cation, the C-I bond length is longer, suggesting that less electron density is donated from the SiPr to form the C-I bond. Therefore, more of the electron density is localized closer to the carbon nucleus. This electron density repels the C-N bonds, resulting in a smaller bond angle. This effect is even more prominent in the SiPr•ICC(TMS) compound. Since a weaker interaction and a longer C-I bond length is observed, it suggests more electron density is centered on the carbenic carbon, repelling the C-N bonds and resulting in an even smaller N-C-N bond angle.

Table 9: Comparison of the carbene N-C-N bond angles in all of the isolated compounds.

Compound	**N-C-N Bond Angle (°)**
SiPr•ICC(TMS)	106.6(2)
[SiPr-I-SiPr]I•$[ICCl]_2$	108.7(5)
[SiPr-I]I	112.5(3)
[SiPr-I]I•ICCl•I[I-SiPr]	112.7(5)
[SiPr-I]I•I_2CCI_2•I•[SiPr-I]	113.0(4)
[SiPr-H]I	113.3(2)
$[SiPr\text{-}I]_2$•$[I]_{16}$	113.9(7)

Note: Atom numbering as described previously.

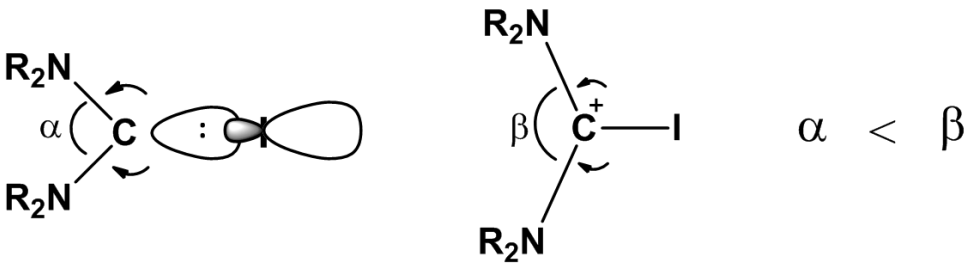

Figure 22: Illustration of the relaxation of the N-C-N bond angle with increased covalent character of the C-I bond.

3.0 Conclusion

SiPr and ICC(TMS) were successfully combined in a 1:1 ratio, and the resulting product has been shown to exhibit a XB interaction. The compound was completely characterized using a combination of liquid and solid state NMR spectroscopy, IR spectroscopy, MP, EA, and X-ray crystallography. Attempts to isolate the bis-adduct of SiPr to ICCI were unsuccessful. Novel compounds, [SiPr-I]I and [SiPr-I]I•ICCI•I[I-SiPr], were isolated and characterized using NMR spectroscopy, IR spectroscopy, MP, and X-ray crystallography. The novel compounds, [SiPr-I]I•I_2CCI_2•I[SiPr-I], [SiPr-I-SiPr]I•$[ICCI]_2$, and $[SiPr\text{-}I]_2$•$[I]_{16}$, were also isolated and characterized using X-ray crystallography. The saturated NHC, SiPr, was shown to behave as both a XB acceptor and also to bond to iodide, creating a [SiPr-I] halogen bond donor. Comparison of the structural results supported the idea that iodine can act as both a XB donor and acceptor. In one case, [SiPr-I]I•I_2CCI_2•I[SiPr-I], the phenyl ring of SiPr was shown to interact electrostatically through a π-type interaction with iodine.

4.0 Future Work

It is likely that SiPr•ICCTMS is an intermediate in many of the mechanisms that produced the isolated compounds. However, the actual pathways are still largely unknown. Now that SiPr•ICC(TMS) can be prepared with relative ease, its reactions with SiPr, I_2, and I^- should offer valuable information into how the isolated compounds are actually being formed. Complete characterization is also needed for the compounds for which only X-ray crystallography has been obtained so far.

It would be interesting to see how changing the nature of C-I bond being inserted into the [SiPr-I]I structure, i.e. using an sp^3-hybridized or an aromatic carbon in the C-I bond, would affect the structures being formed. Now that we can readily make [SiPr-H]I, interacting it with small iodine-containing molecules would also be of interest. If new structures were characterized, it would also likely give us more insight into the nature of the compounds formed with [SiPr-I]I.

Work should be done to investigate the abilities of [SiPr-I]I•ICCI•I[I-SiPr] and [SiPr-I]I•I_2CCI_2•II[I-SiPr] to act as oxidizing agents. Some tests have been run on each compound, but these have been very preliminary. It would also be beneficial to see if the number of iodide ions inserted between [SiPr-I] and ICCI could be increased. If more than one iodide ion could be inserted, the likelihood of the compound behaving as an oxidizing agent may increase.

5.0 Experimental

5.1 General Procedures

All preparations were carried out under an inert nitrogen atmosphere in an mBraun glovebox, unless otherwise stated. Nitrogen (>99.998%) was provided by Praxair Inc. Anhydrous benzene (99.8%), anhydrous N,N-dimethylformamide (99.8%), N-iodosuccinimide (95%), anhydrous acetonitrile (99.8%), ethyltrimethylsilane (98%), dry sodium hydride (95%), reagent grade potassium *tert*-butoxide (95%), 1-iodo-2-(trimethylsilyl)acetylene (97%), HPLC grade 1,2-dichloroethane, reagent plus grade *N*,*N*-diisopropylethylamine (≥99%), anhydrous 1 ppm butylated hydroxytoluene (BHT) in diethyl ether (≥99.7%), anhydrous BHT, ACS reagent grade diethyl ether (≥99.0%), 2,6-diisopropylaniline (97%), anhydrous triethylorthoformate (98%), and glacial acetic acid were purchased from Sigma-Aldrich. Reagent grade tetrahydrofuran (THF), dichloromethane (DCM), hexanes and toluene were purchased from Caledon Laboratory Chemicals. The solvents were purified using an mBraun solvent still and stored over 4 Å molecular sieves prior to use. Benzene-d_6 (d: 99.5%) and acetonitrile-d_3 (d: 99.8%) were purchased from Cambridge Isotope Laboratories and were opened and stored under a nitrogen environment.

5.2 Analytical Techniques

Infrared spectra were collected as KBr pellets with a Bruker Vertex 70 Infrared Spectrometer and the data was processed using the OPUS 6.0 software suite.

The ^{1}H NMR spectra were collected using a Bruker Ultrashield 300 MHz NMR spectrometer with a 7.05 Tesla magnet. ^{13}C NMR was carried out at 75 MHz, with the

same instrument. Samples were prepared by dissolving a small amount of sample into the minimum about of deuterated solvent, under an inert atmosphere. ^{1}H NMR spectra were referenced to the residual solvent peaks downfield of trimethylsilane. The data was processed using Bruker TOPSPIN 1.3.

Elemental analyses (EA) were performed on a Perkin Elmer CHN Analyzer 2400 Series II. Prior to data acquisition, standard calibration was conducted with acetanilide supplied by Perkin Elmer. All EA data acquisition was carried out by Patricia Granados of the Centre for Environmental Analysis and Remediation at Saint Mary's University.

The melting points were measured using a Mel-Temp melting point apparatus (with a heating rate of ca. 5°C min^{-1}) and are uncorrected. The samples were placed in a capillary tube, under an inert atmosphere, and then sealed.

5.3 X-ray Crystallography

The crystal chosen for each determination was attached to the tip of a 400 μm MicroLoop with paratone-N oil. Measurements were made on a Bruker APEXII CCD equipped diffractometer (30 mA, 50 kV) using monochromated Mo Kα radiation (λ = 0.71073 Å) at 125 K.[54] The initial orientation and unit cell were indexed using a least-squares analysis of a random set of reflections collected from three series of 0.5° ω-scans, 15 seconds per frame and 12 frames per series, that were well distributed in reciprocal space. For data collection, four ω-scan frame series were collected with 0.5° wide scans, 30 second frames and 366 frames per series at varying φ angles (φ = 0°, 90°, 180°, 270°). The only exception was made in the data collection for [SiPr-I-SiPr]I · 2ICCl · C_6H_6 where each frame was collected for 40 seconds. The crystal to detector distance

was set to 6 cm and a complete sphere of data was collected. Cell refinement and data reduction were performed with the Bruker SAINT[55] software, which corrects for beam inhomogeneity, possible crystal decay, Lorentz and polarisation effects. A multi-scan absorption correction was applied (SADABS[56]). The structures were solved using SHELXT-2014[57] and were refined using a full-matrix least-squares method on F^2 with SHELXL-2014.[57] All refinements were unremarkable. The non-hydrogen atoms were refined anisotropically. Hydrogen atoms bonded to carbon were included at geometrically idealized positions and were not refined. The isotropic thermal parameters of the hydrogen atoms were fixed at $1.2U_{eq}$ of the parent carbon atom or $1.5U_{eq}$ for methyl hydrogens.

5.4 Synthetic methods

5.4.1 Preparation of N,N-Bis(2,6-diisopropylphenyl)formamidine[47]

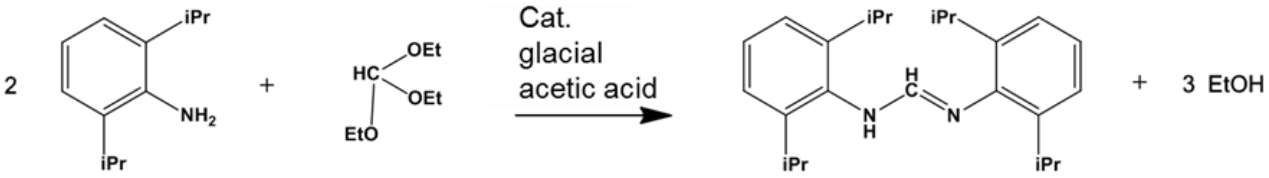

Note: this reaction was completed on the benchtop, not under an inert atmosphere.

2,6-Diisopropylaniline (35.89 g, 202 mmol, 2 equiv.), triethylorthoformate (15 g, 101 mmol, 1 equiv.) and glacial acetic acid (1.215 g, 20.2 mmol, 0.2 equiv.) were added to a 500 mL round-bottomed flask and the flask was fitted with a distillation apparatus. The reaction flask was then heated to 160°C for 20 hours. Ethanol was collected as it distilled. After 20 hours, the amount of diethyl ether necessary to dissolve the product was added to the reaction flask. This was then transferred to a 1000 mL separatory funnel and diethyl ether was added to a total volume of 800 mL. A saturated solution of sodium bicarbonate

(100 mL) was added to the funnel. The ether layer was separated and treated with sodium sulfate. The solution was then added to a 1000 mL round bottomed flask and the solvent was removed under vacuum using a rotary evaporator. White solid was obtained and washed with cold hexane to produce the white fluffy product.

5.4.2 Preparation of [SiPr-H]Cl[48]

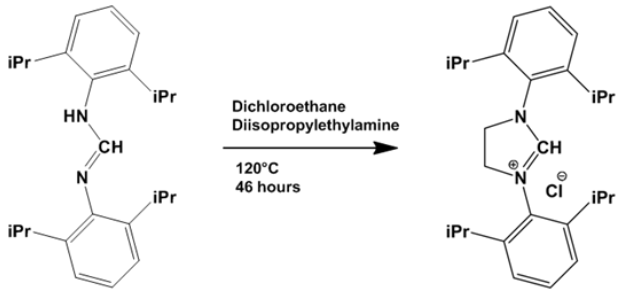

N,N-(2,6-Diisopropylphenyl)formamidine (14.493 g, 39.8 mmol, 1 equiv.) and dichloroethane (39.33 g, 397.5 mmol, 10 equiv.) were added to a 500 mL Schlenk bomb and stirred. To the stirred solution diisopropylethylamine (5.65 g, 43.7 mmol, 1.1 equiv.) was subsequently added. The Schlenk bomb was sealed under static vacuum and then heated to 120°C using a silicon oil bath. The reaction was left to proceed for 46hrs. The reaction flask was removed from the heat and allowed to cool to room temperature, during which time dark pink crystals formed. Excess dichloroethane was removed under vacuum. The product was washed with 3 × 75 mL of boiling toluene and filtered through a glass frit. A pale pink product was obtained. (yield 9.196 g, 54.3%) ^{1}H NMR (300 MHz, $CDCl_3$, δ ppm) 1.26 - 1.29 (d, 2-C*H*$_3$, 12 H), 1.40 – 1.43 (d, 6-C*H*$_3$, 12 H), 3.04 (m, 2,6-C*H*, 4 H), 4.88 (s, NC*H*$_2$, 4H), 7.28 - 7.31 (m, 3,5-Ar*H* 4 H), 7.49 - 7.52 (m, 4-Ar*H*, 2 H), 8.39 (s, NC*H*N, 1H).

5.4.3 Preparation of SiPr[49]

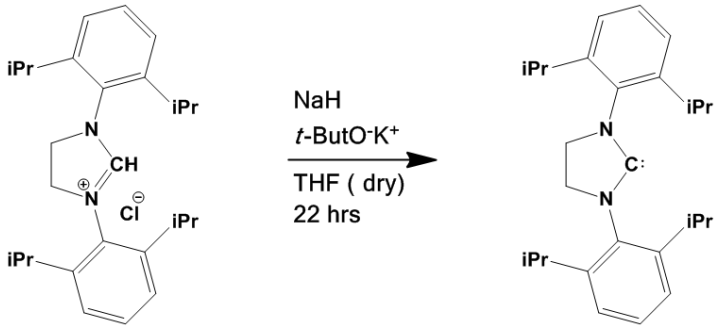

[SiPr-H] • Cl (7.71 g, 18.1 mmol, 1 equiv.) was added to a ca. 175 mL of THF in a 250 mL Schlenk flask and stirred. NOTE: Sodium hydride is very reactive and its reaction with [SiPr-H]Cl is quite exothermic, care should be taken when adding the reagent to the reaction flask. Sodium hydride (1.74 g, 72.4 mmol, 4 equiv.) and potassium *tert*-butoxide (0.203, 1.81 mmol, 0.1 equiv.) were added to the reaction flask and left for 22 hrs. The solution was then filtered through Celite and the THF was removed in vacuo. The remaining solid was triturated with dry hexanes and dried in vacuo. (yield ca. 2g) ^{1}H NMR (300 MHz, C_6D_6, δ ppm) 1.28 - 1.30 (d, 2-C*H*$_3$, 12 H), 1.32 – 1.34 (d, 6-C*H*$_3$, 12 H), 3.28 (m, 2,6-C*H*, 4 H), 3.37 (s, NC*H*$_2$, 4H), 7.17 - 7.19 (m, 3,5-Ar*H* 4 H), 7.24 - 7.29 (m, 4-Ar*H*, 2 H).

5.4.4 Preparation of ICCI[53]

*****CAUTION** Diiodoactylene has been reported to decompose violently at temperatures between 80°C and 130°C or due to shock. Therefore, extreme care should be taken when dealing with it in the solid state and for safety reasons it should be stored in solution as a precaution.***

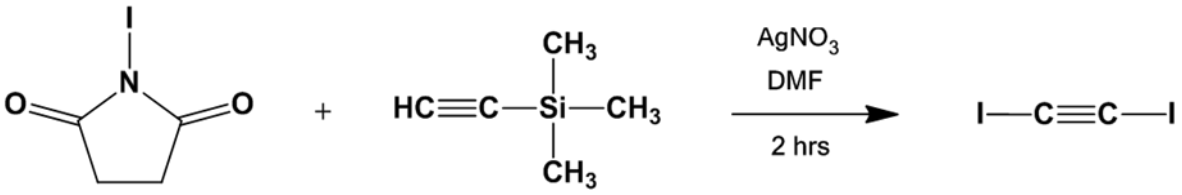

The following synthesis was carried out under an inert atmosphere, in a glovebox. *N*-iodosuccinimide (2.52g, 11.22 mmol, 2.2 equiv.) was weighed out and added to a 50 mL round-bottomed flask along with silver nitrate (0.085g, 0.50 mmol, 0.098 equiv.). HCC(TMS) (0.50g, 5.1 mmol, 1 equiv.) was weighed out and added to 15 mL of DMF in a 20 mL scintillation vial. This solution was then added to the round-bottomed flask and stirred for 1 hr. The resulting solution was then treated with 20-30 mL of deionized water and extracted with 3 x 10 mL aliquots of diethyl ether. It was dried with magnesium sulfate. The solution was gravity filtered and the product was left in diethyl ether solution.

5.4.5 Synthesis of SiPr • ICCTMS

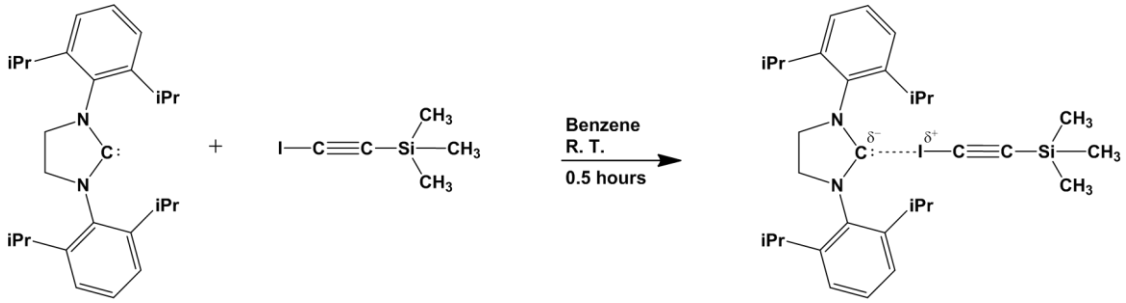

The reaction was carried out under an inert atmosphere, in a glovebox. SiPr (130 mg, 0.33 mmol, 1 equiv.) was weighed out in a 20 mL scintillation vial and dissolved in 6 mL of hexane. This solution was then added to a 50 mL Schlenk flask equipped with a stir bar. ICC(TMS) (74 mg, 0.33 mmol, 1 equiv) was weighed out in a 20 mL scintillation vial and 6 mL of hexane was added to it. This solution was added in a dropwise fashion to the stirring solution in the 50 mL Schlenk flask. Once the ICC(TMS) addition was

complete, the flask was capped and the reaction mixture was allowed to stir for 30 minutes. The reaction flask was kept sealed and placed in a freezer where clear, colourless, rectangular crystals formed after 2-3 hrs. (yield ca. 150 mg) mp. 128-130°C (dec). ^{1}H NMR (300 MHz, C_6D_6, δ ppm) 1.20 (d, 2-C*H*$_3$, 12 H), 1.38 (d, 6-C*H*$_3$, 12 H), 3.10 (m, 2,6-C*H*, 4 H), 3.77 (s, NC*H*$_2$, 4H), 7.09 - 7.14 (m, 3,5-Ar*H* 4 H), 7.19 - 7.26 (m, 4-Ar*H*, 2 H). ^{13}C NMR (75 MHz, C_6D_6, δ ppm) 23.92 (s, CH(*C*H$_3$)$_2$), 24.67 (s, CH(*C*H$_3$)$_2$), 28.57 (s, *C*H(CH$_3$)$_2$), 21.06 (s, IC*C*Si), 52.97 (s, N*C*H$_2$), 98.03 (s, I*C*CSi), 123.89 (s, *meta*-*C*), 128.62 (s, *ortho*-*C*), 137.02 (s, ipso-*C*), 146.64 (s, *para*-*C*), 225.14 (s, N*C*N). IR (KBr, cm^{-1}) 2964 (s), 2868 (m), 2071 (w), 1675 (w), 1589 (vw), 1460 (s), 1422 (m), 1325 (w), 1263 (m), 1242 (m), 1180 (w), 1104 (w), 1057 (w), 936 (vw), 839 (s), 804 (m), 757 (s), 710 (m), 614 (vw).

5.4.6 Synthesis of [SiPr—I] • I • ICCI • I • [I-SiPr]

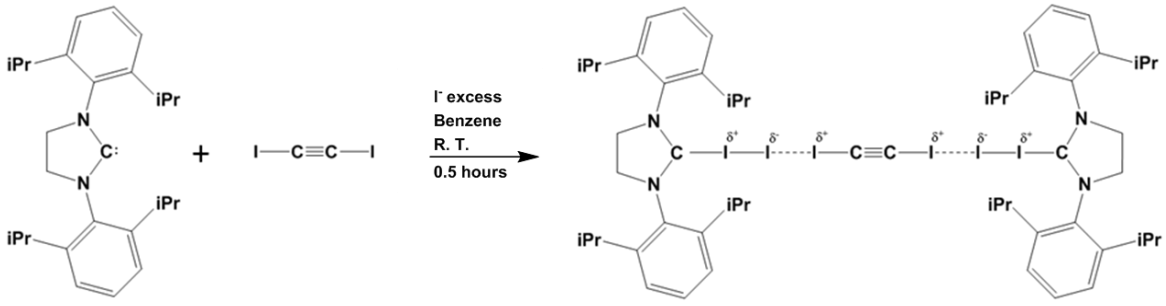

The reaction was carried out under an inert atmosphere, in a glovebox. Due to the unstable nature of ICCI, its yield was never obtained. Thus, the equivalency of the amounts of SiPr and ICCI added in this reaction are unclear. SiPr (0.10 g, 0.26 mmol) was added to a 6 mL of benzene in a 50 mL Schlenk flask at room temperature and stirred. 8.0 mL of the ICCI / benzene solution was added to the flask and left to react for 30 minutes. The precipitate that was formed was collected by gravity filtration. This solid

was then dissolved in a minimum amount of acetonitrile. Crystals formed after slow evaporation of the solvent. (yield ca. 100 mg) mp. 240-244°C (dec). ^{1}H NMR (300 MHz, CD_3CN, δ ppm) 1.36 (d, 2-C*H*$_3$, 24 H), 1.38 (d, 6-C*H*$_3$, 24 H), 2.99 (m, 2,6-C*H*, 8 H), 4.36 (s, NC*H*$_2$, 8H), 7.43 - 7.49 (m, 3,5-Ar*H*, 8 H), 7.58 - 7.65 (m, 4-Ar*H*, 4 H). ^{13}C NMR (75 MHz, C_6D_6, δ ppm) 23.37 (s, CH(*C*H$_3$)$_2$), 24.20 (s, CH(*C*H$_3$)$_2$), 28.94 (s, *C*H(CH$_3$)$_2$), 53.86 (s, N*C*H$_2$), 125.40 (s, *meta*-*C*), 131.45 (s, *ortho*-*C*), 132.65 (s, ipso-*C*), 146.57 (s, *para*-*C*), no N*C*N resonance detected. IR (KBr, cm^{-1}) 2964 (vs), 2927 (m), 2868 (m), 1703 (vw), 1627 (vw), 1589 (w), 1536 (vs), 1460 (m), 1270 (s), 1103 (w), 1049 (m), 1016 (m), 917 (w), 805 (s), 757 (w), 671 (vw), 449 (vw).

5.4.7 Synthesis of [SiPr—I]I

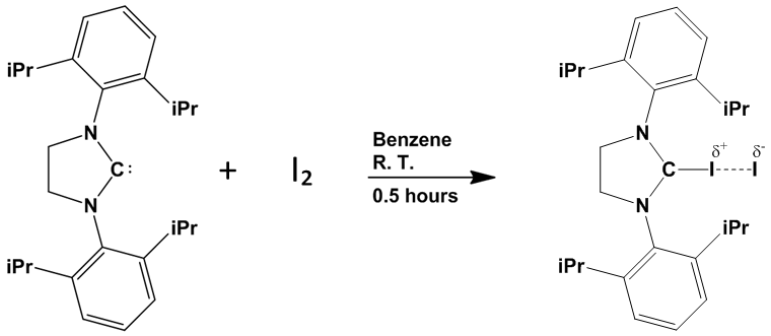

The reaction was carried out under an inert atmosphere, in a glovebox. SiPr (0.10g, 0.256 mmol, 1 equiv.) was weighed out and added to a 50 mL Schlenk flask, then dissolved in 4 mL of benzene and stirred. I_2 (0.065 g, 0.256 mmol, 1 equiv.) was weighed out and dissolved in 4 mL of benzene. The iodine/benzene solution was added dropwise to the stirring SiPr/benzene solution. The reaction was left to proceed for 15 minutes and then the solvent was removed in vacuo. This crude solid was dissolved in acetonitrile and clear, colourless, rectangular crystals were obtained from the resulting solution by slow evaporation. (yield ca. 100 mg) mp. 276-278°C (dec). ^{1}H NMR (300 MHz, CD_3CN, δ ppm)

1.34 (d, 2-C*H*$_3$, 12 H), 1.36 (d, 6-C*H*$_3$, 12 H), 2.96 (m, 2,6-C*H*, 4 H), 4.36 (s, NC*H*$_2$, 4H), 7.41 - 7.47 (m, 3,5-Ar*H*, 4 H), 7.55 - 7.63 (m, 4-Ar*H*, 2 H). ^{13}C NMR (75 MHz, C_6D_6, δ ppm) 23.39 (s, CH(*C*H$_3$)$_2$), 24.18 (s, CH(*C*H$_3$)$_2$), 28.94 (s, *C*H(CH$_3$)$_2$), 53.80 (s, NCH$_2$), 125.38 (s, *meta*-*C*), 131.40 (s, *ortho*-*C*), 132.68 (s, ipso-*C*), 146.57 (s, *para*-*C*). no N*C*N resonance detected. IR (KBr, cm^{-1}) 2966 (s), 2925 (m), 2867 (m), 1589 (w), 1536 (vs), 1463 (m), 1283 (s), 1180 (vw), 1103 (vw), 1056 (w), 1017 (w), 808 (m), 759 (w).

5.4.8 Synthesis of [SiPr-I-SiPr] • I • (ICCl)$_2$

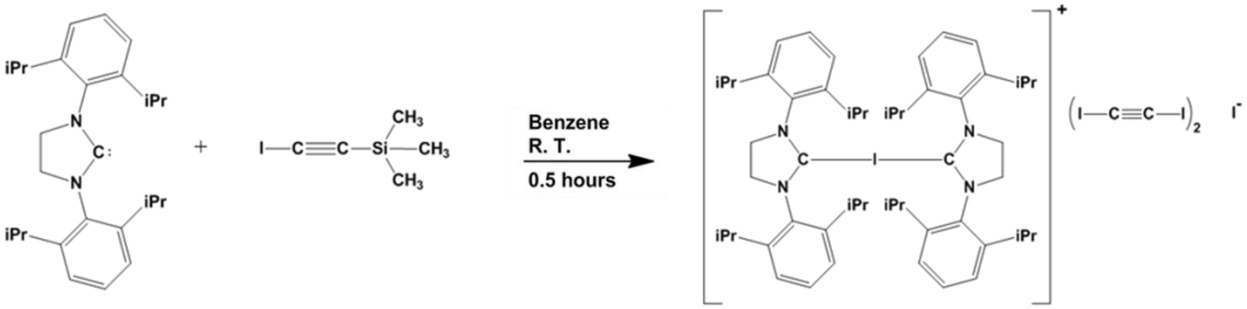

The reaction was carried out under an inert atmosphere in a glovebox. SiPr (150 mg, 0.38 mmol, 1 equiv.) was weighed out in a 20 mL scintillation vial and dissolved in 6 mL of either benzene. This solution was then added to a 50 mL Schlenk flask equipped with a stir bar. ICC(TMS) (86 mg, 0.38 mmol, 1 equiv) was weighed out in a 20 mL scintillation vial and 6 mL of either benzene was added to it. This solution was added in a dropwise fashion to the stirring solution in the 50mL Schlenk flask. The reaction was left to proceed for 30 minutes at room temperature. Crystals formed after slow evaporation from the same benzene solution.

5.4.9 Synthesis of [SiPr-I]$_2$ • [I]$_{16}$

The isolation of this compound came from an attempt to isolate the [SiPr-I]I$_3$ compound. About 50 mg of the crystals of [SiPr-I]I were added to a 20 mL scintillation vial, dissolved

in acetonitrile, and stirred. In a separate scintillation vial an excess of iodine was dissolved in acetonitrile; this was added dropwise to the stirring solution. The reaction was allowed to procced for 30 minutes. The remaining solution was then left for slow evaporation, where crystals gradually appeared.

5.4.10 Synthesis of [SiPr-I] • I • I_2CCl_2 • I • [SiPr-I]

It is likely that the ICCI solution we synthesized contained excess iodide. Therefore attempts were made to quench the solution of the iodide with small additions of SiPr. SiPr was added in small amount (ca. 10 mg) to the ICCI/diethyl ether solution. A precipitate formed immediately and the remaining solution was decanted. The same procedure was continued until no precipitate formed upon addition of SiPr. The precipitates were dissolved in acetonitrile where clear, pale yellow, thin rod-like crystals formed from slow evaporation.

6.0 References

1. Tro, N. J. *Chemistry A Molecular Approach*; Pearson Prentice Hall: New Jersey, **2008**; pp 1017.

2. Sykes, P. A Guidebook to Mechanism in Organic Chemistry; Longman: England, **1986**. pp 96−100.

3. Gilday, L. C.; Robinson, S. W.; Barendt, T. A.; Langton, M. J.; Mullaney, B. R.; Beer, P.D. *Chem. Rev*. **2015**, 115, 7118−7195.

4. Metrangelo, P.; Meyer, F.; Pilati, T.; Resnati, G.; Terraneo, G. *Angew. Chem. Int. Ed.* **2008**, 47, 6114−6127.

5. Metrangelo, P.; Resnati, G. *Chem. Eur. J.* **2001**, 7, 2511−2519.

6. Colin, M. *Ann. Chim.* **1814**, 91, 252−272.

7. Guthrie, F. *J. Chem. Soc.* **1863**, 16, 239−244.

8. Dehn, W. M. *J. Am. Chem. Soc.* **1911**, 33, 1598−1601

9. Benasi, H. A.; Hildebrand, J. H. *J. Am. Chem. Soc.* **1948**, *70*, 2832−2833.

10. (a) Groth, P.; Hassel, O. *Acta Chem. Scand.* **1965**, 19, 1733−1740. (b) Hassel, O.; Stromme, K. O. *Nature* **1958**, 182, 1155−1156. (c) Groth, P.; Hassel, O. *Acta Chem. Scand.* **1964**, 18, 402−408.

11. Bent, H. A. Chem. Rev. **1968**, 68, 587-648.

12. Dumas, J. M.; Peurichard, H.; Gomel, M. J. *Chem. Res., Synop.* **1978**, 54−55.

13. Metrangelo, P.; Resanti, G. *Cryst. Growth Des.* **2012**, 12, 5835−5838.

14. Clarke, T.; Hennemann, M.; Murray, J. S.; Politzer, P. *J. Mol. Model.* **2007**, 13, 291−296.

15. Metrangolo, P.; Neukirch, H.; Pilati, T.; Resnati, G. *Acc. Chem. Res.* **2005**, 38, 386−395.

16. Murray, J. S.; Paulsen, K.; Politzer, P. *Proc. Indian Acad. Sci. (Chem. Sci*.) **1994**, 106, 267−275.

17. Metrangolo, P.; Pilati, T.; Terraneo, G.; Biella, S.; Resnati, G. *CrystEngComm* **2009**, 11, 1187−1196.

18. Pan, F.; Beyeh, N. K.; Rissanen, K. *J. Am. Chem. Soc.* **2015**, 137, 10406−10413.

19. Virkki, M.; Tuominen, O.; Forni, A.; Saccone, M.; Metrangelo, P.; Resnati, G.; Kauranen, M.; Priimagi, A. *J. Mater. Chem. C.* **2015**, 3, 3003−3006.

20. Jungbauer, S. H.; Walter, S. M.; Schindler, S.; Rout, L.; Kniep, F.; Huber, S.M. *Chem. Commun.* **2014**, 50, 6281−6284.

21. Lu, Y.; Wang, Y.; Zhu, W. *Phys. Chem. Chem. Phys.* **2010**, 12, 4543−4551.

22. Persch, E.; Dumele, O.; Diederich, F. *Angew. Chem. Int. Ed.* **2015**, 54, 3290−3327.

23. Nguyen, H. L.; Horton, P. N.; Hursthouse, M. B.; Legon, A. C.; Bruce, D. W. *J. Am. Chem. Soc.* **2004**, 126, 16−17.

24. Sun, A.; Goroff, N. S.; Lauher, J. W. *Science* **2006**, 312, 1030−1034.

25. Solomons, T. W. G.; Fryhle, C. B. Organic Chemistry, 9th ed.; Wiley & Sons: New Jersey, **2008**; pp 72.

26. Bourissou, D.; Guerret, O.; Gabbaï, F. P.; Bertrand, G. Chem. Rev. **2000**, 100, 39−92.

27. Herrmann, W. A. *Angew. Chem. Int. Ed.* **2002**, 41, 1290−1309.

28. Nelson, D. J.; Nolan, S. P. N-Heterocyclic Carbenes. In N-Heterocyclic Carbenes Effective Tools for Organometallic Synthesis; Nolan, S. P., Ed.; Wiley-VCH: Weinheim, Germany, **2006**; pp 1.

29. Wanzlick, H. W. *Angew. Chem., Int. Ed. Engl.* **1962**, 1, 75−80.

30. Arduengo, A. J.; Harlow, R. L.; Kline, M. *J. Am. Chem. Soc.* **1991**, 113, 361−363.

31. Diez-Gonzalez, S.; Marion, N.; Nolan, S. P. *Chem. Rev.* **2009**, 109, 3612−3676.

32. Dixon, D. A.; Arduengo, A. J. *J. Phys. Chem.* **1991**, 95, 4180−4182.

33. Arduengo, A. J.; Dixon, D. A.; Kumashiro, K. K.; Lee, C.; Power, W. P.; Zilm, K. W. *J. Am. Chem. Soc.* **1994**, 116, 6361−6367.

34. Heinemann, C.; Müller, T.; Apeloig, Y.; Schwarz, H. *J. Am. Chem. Soc.* **1996**, 118, 2023−2038.

35. Laurence, C.; Queignec-Cabanetos, M.; Dziembowska, T.; Queignec, R.; Wojtkowiak, B. *J. Am. Chem. Soc.,* **1981**, 103, 2567−2573.

36. Gagnaux, P.; Susz, B. P. *Helv. Chin. Acta.* **1960**, 43, 948−956.

37. Holmesland, O.; Romming, C. *ibid.* **1966**, 20, 2601.

38. Moss, W. N.; Goroff, N. S. *J. Org. Chem.* **2005**, 70, 802−808.

39. Webb, J. A.; Klijn, J. E.; Hill, P. A.; Bennett, J. L.; Goroff, N. S. *J. Org. Chem.* **2004**, 69, 660−664.

40. Dumele, O.; Wu, D.; Trapp, N.; Goroff, N.; Diederich, F. *Org. Lett.* **2014**, 16, 4722−4725.

41. Cavallo, G.; Metrangolo, P.; Milani, R.; Pilati, T.; Priimagi, A.; Resnati, G.; Terraneo, G. *Chem. Rev.* **2016**, 116, 2478−2601.

42. Li, B.; Zang, S. Q.; Wang, L. Y.; Mak, T. C. W. *Coord. Chem. Rev.* **2016**, 308, 1−21.

43. Desiraju, G. R.; Parthasarathy, R. *J. Am. Chem. Soc.* **1989**, 111, 8725−8726.

44. Arduengo, A. J.; Kline, M.; Calabrese, J. C.; Davidson, F. *J. Am. Chem. Soc*. **1991**, 113, 9704−9705.

45. Arduengo, A. J.; Tamm, M.; Calabrese, J. C. *J. Am. Chem. Soc.* **1994**, 116, 3625−3626.

46. Lv, H.; Zhuo, H. Y.; Li, Q. Z.; Yang, X.; Li, W. Z.; Cheng, J. B. *Molecular Physics*, **2014**, 112, 3024−3032.

47. Krachulic, K. E.; Enright, G. D.; Parvez, M.; Roesler, R. *J. Am. Chem. Soc.* **2005**, 127, 4142−4143.

48. Kuhn. K. M.; Grubbs, R. H. *Org. Lett.* **2008**, 10, 2075−2077.

49. Bantreil, X.; Nolan, S. P. *Nature Protocols*, **2011**, 6, 69−77.

50. Mercury CSD 3.5.1. Macrae, C.F.; Bruno, I.J.; Chisholm, J.A.; Edgington, P.R.; McCabe, P.; Pidcock, E.; Rodriguez-Monge, L.; Taylor, R.; van de Streek, J.; Wood, P.A. J. Appl. Cryst. **2008**, 41, 466−470.

51. Ghassemzadeh, M.; Harms, K.; Dehnicke, K. *Chem. Ber.* **1996**, 259−262.

52. Acetylene; MSDS No. 200-816-9 [Online]; Linde Canada Ltd.: Mississauga, ON. Mar 11, 2015. http://www.lindecanada.com/internet.lg.lg.can/en/images/Acetylene_EN135_104283.pdf (accessed Apr 2, 2016).

53. Perkins, C.; Libri, S.; Adams, H.; Brammer, L. *CrystEngComm* **2012**, 14, 3033−3038.

54. APEX II (Bruker, 2008) Bruker AXS Inc., Madison, Wisconsin, USA.

55. SAINT (Bruker, 2008) Bruker AXS Inc., Madison, Wisconsin, USA.

56. SADABS (Bruker, 2009) Bruker AXS Inc., Madison, Wisconsin, USA.

57. Sheldrick, G.M. (2008) Acta Cryst., A64, 112-122; Sheldrick, G.M. (2015) Acta Cryst., A71, 3-8; Sheldrick, G.M. (2015) Acta Cryst., C71, 3−8.

58. Knop, O.; Choi, S. C. Hamilton, D. C. *Can. J. Chem.* **1992**, 70, 2574−2601.

59. Arduengo, A. J.; Krafczyk, R.; Schmutzler, R. *Tetrahedron* **1999**, 55, 14523−14534.

60. Jahnke, E.; Weiss, J.; Neuhaus,S.; Hoheisel, T. N.; Frauenrath, H. *Chem. Eur. J.* **2009**, 15, 388−404.